Bull. Inst. Chem. Res., Kyoto Univ., Vol. 73, No. 1, 1995

Qualitative Analysis of 4-rod RFQ Resonators

Valeri KAPIN*,†, Makoto INOUE*,
Yoshihisa IWASHITA* and Akira NODA*

Received February 6, 1995

The 4-rod RFQ resonator is simulated by a resonant circuit based on the four-conductor shielded transmission line (4CSTL). The normal mode analysis for TEM waves is applied to a certain model structure. The mathematical derivations of the normal modes propagating in the 4CSTL and their physical interpretation are described. Some examples to reconstruct the RFQ fields from the results of the normal mode analysis are in good agreement with the 3-D calculations by MAFIA code.

KEYWORDS: Linear accelerator/ 4-rod RFQ resonator/ Equivalent circuits/ TEM wave/ Normal mode/ Four-conductor shielded transmission line

1. INTRODUCTION

Many different configurations of the so-called 4-rod Radio-Frequency Quadrupole (RFQ) have been constructed for the linear accelerators[1-38]. The 4-rod RFQ resonator consists of four longitudinal electrodes connected with a tank by supporting posts as shown in Fig. 1.

Some equivalent circuits have been developed[1-4,6-8,10-14,21,23,26,28,39-46], but there is no general method proposed to study any configurations of the 4-rod RFQ resonators. This circumstance makes their comparative analysis difficult and impedes an optimal selection of their configuration at the given conditions. In this paper we will present a generalized modeling approach which can be applied for a wide family of the 4-rod RFQ resonators.

Our method is the usual approach for modeling of a microwave-transmission system as an equivalent circuit which is composed of sections of uniform transmission lines jointed together through coupling networks. The representation with equivalent circuit is helpful to understand intuitively the resonator. It allows to predict their behavior and leads to systematic design, study, and testing[47,48].

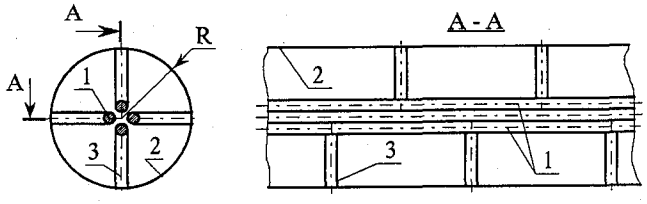

Fig. 1. General concept of the 4-rod RFQ resonator: 1 is a quadrupole electrode; 2 is a tank; 3 is an electrode-supporting post.

* Valeri Kapin, 井上 信, 岩下芳久, 野田 章: Accelerator Laboratory, Nuclear Science Research Facility, Institute for Chemical Research, Kyoto University, Uji, Kyoto 611, Japan.
† On leave from Moscow Engineering Physics Institute.

Our approach can be considered as an extension of the conventional transmission line theory based on the concepts of distributed parameters. In this case, a real 3-D electrodynamics problem is reduced to an equivalent-circuit problem. So far, all studies had made some specific assumptions which came from only the particular geometry of each investigated resonator. Our method includes some numerical calculations of 2-D problems to study 3-D problems without any specific assumptions within 2-D problem. It allows to extend the abilities of the equivalent-circuits modeling to the application such as to study the 4-rod RFQ.

The 4-rod RFQ resonator can be simulated by a resonant circuit[49,50], which consists of four-conductor shielded transmission lines (4CSTL) loaded by sets of the impedance corresponding to the transverse supports (Fig. 2). It is assumed that only TEM waves propagate along all conductors of the resonant circuit. The standing waves defining the mode of the resonance oscillation is the superposition of the *waveguide* modes propagating on the transmission lines. This interrelation between the resonance and waveguide modes characterizes a resonance mode through the corresponding waveguide modes. For example, the accelerating system for electron linac can be treated as a sequence of small cavities with TM_{01} waveguide modes. The Alvarez structure, the Four-vane RFQ resonator and Double-H-resonator can be represented as single cavities based on the TM_{01}, TE_{21}, TE_{11} waveguide modes, respectively[1,51].

In order to study the 4-rod RFQ resonators, we should consider in detail the behavior of the corresponding waveguide of the 4CSTL. In this case we have used conceptions of the normal TEM modes propagating in the multi-conductor transmission line system. It is shown that purely mathematically derived normal propagating modes have clear physical interpretations. Some qualitative results based on the normal TEM mode analysis for the 4-rod RFQ resonators are presented in this paper. It is demonstrated how a field of the resonator can be reconstructed by a normal mode combination.

In section 2 a review of constructions of the 4-rod RFQ resonators is presented. The general behaviors of the multi-conductor TEM transmission lines are described in section 3. The method of normal TEM modes in the 4CSTL is presented in section 4. The fifth section is devoted to the qualitative considerations of the 4-rod resonators based on our method. Examples of the transformation from the 4CSTL to 4-rod RFQ resonators are given. The examples of resonators have different normal mode contents. The results are compared with the 3-D calculations by MAFIA code.

2. THE 4-ROD RFQ RESONATOR AS A CAVITY WITH THE TEM WAVES

Although the 4-rod RFQ resonator contains only two kinds of principal elements : electrodes and posts, there can be a lot of configurations. The longitudinal profile is usually uniform, but

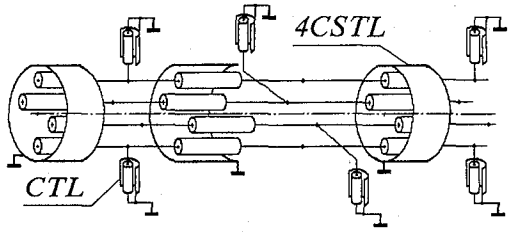

Fig. 2. The equivalent circuit of the 4-rod RFQ resonator.

Split-Coaxial Resonator (SCR) with "spear-shaped beams" is an example of the non-uniform case. The transverse cross-section of the electrodes can have a simple round geometry or a complicated one with various vane-like shapes. The different kinds of the supporting posts (straight, triangular and cylindrical stems or spiral supports) have been designed.

In this paper we will treat the 4-rod RFQ resonators as cavities with TEM waves, using transmission line theory. Similar approaches were separately applied to drift-tube resonators[59] and for RFQ resonators[2-4,7,8,10-12,40,41]. Here we will develop a general procedure according to our previous studies presented in Refs.[49,50,60-63]. The basic condition for our approach is an assumption that only TEM waves propagate along all conductors. Simulating the 4-rod RFQ by equivalent circuit in Fig. 2 we will assume that the characteristics of resonators are determined by the 4CSTL with TEM standing wave.

The well-known condition for propagation of only TEM waves requires that the transverse physical dimensions of the 4CSTL must be much less than the wavelength λ. In our case it can be formulated as $R/\lambda \ll 1$, where the tank radius R plays a role of such transverse physical dimension. The relation between R/λ and λ of existing 4-rod RFQ resonators is shown in Fig. 3. The above condition seems to be satisfied in the existing 4-rod RFQ resonators.

All resonators presented in Fig. 3 are grouped in the following several types : 1) split-coaxial resonators (SCR) with spear-shaped beams[1,11,12,23]; 2) one module SCR with round rods[7,21] ; 3) 4-rod RFQ with spiral supports[9,16,29] ; 4) the "In-line stems 4-rod RFQ" [1,10,13] (the connection points of all rods with the tank are located at the same longitudinal position) ; 5) the "Alternate

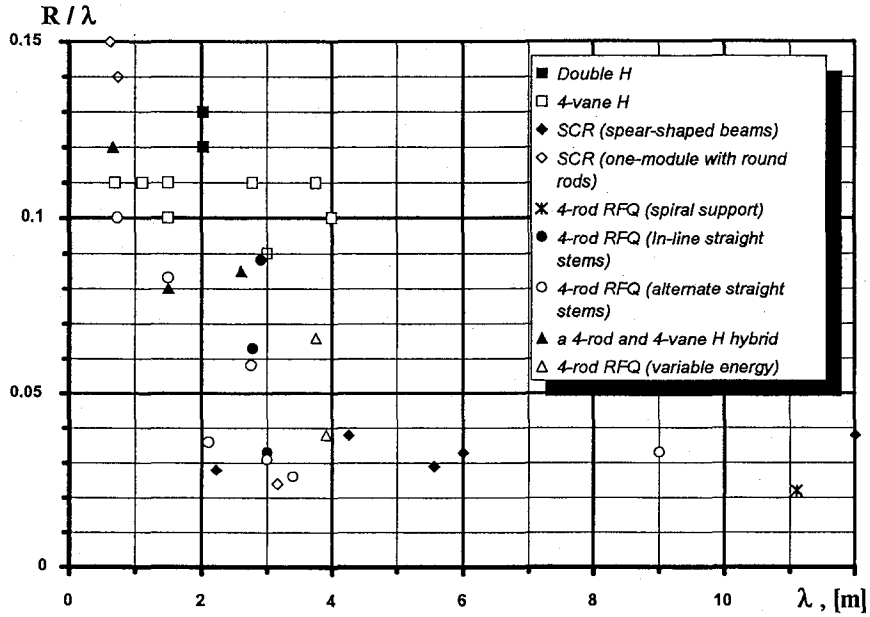

Fig. 3. The ratio of the tank radius R to the wavelength λ for the different RFQ resonators : 1) Double H [1] ; 2) 4-vane H [1] ; 3) SCR (spear-shaped beams) [1, 11, 12, 23] ; 4) SCR (one-module with round rods) [7, 21] ; 5) 7) 4-rod RFQ (spiral supports) [9, 16, 29] ; 6) 4-rod RFQ (In-line straight stems) [1,10,13] ; 7) 4-rod RFQ (alternate straight stems) [17, 18, 20, 24, 28, 37] ; 8) a 4-rod and 4-vane H hybrid [33, 34, 36] ; 9) 4-rod RFQ (variable energy) [22, 25].

stems 4-rod RFQ"[17,18,20,24,28,37] (each set of opposing rods is connected to the tank at the middle of the successive supports of the other set of rods) ; 6) Variable energy 4-rod RFQ[22,25] ; 7) a 4-rod and 4-vane H hybrid[33,34,36,38]. Also in Fig. 3 we show parameters for two main types of H-resonators in which non-TEM waves with longitudinal field component, namely H (TE) waves, can arise in the case of $R/\lambda \geq 0.1$. As shown in Fig. 3, all types of the Four-rod RFQ resonators in meter waveband satisfy condition $R/\lambda \leq 0.1$. At the value of $R/\lambda = 0.1$ there is a border between TEM (4-rod RFQ) resonators and H (TE)-resonators except some kind of resonators in decimetric waveband, where a possible alternative for H-resonators can be considered. Under these conditions, we can recognize the main limitation of presented modeling method. For some cases the method may give correct quantitative and qualitative results, but for other cases it becomes only a qualitative model. It depends on the order of difference between an ideal TEM field and a real 3-D field in the resonator. But main purpose of the present work is not get numerical results but qualitative study.

3. DESCRIPTION OF TEM WAVES IN THE 4CSTL

In this section we will introduce some features of a mathematical description of the TEM wave propagation in the 4CSTL. The general behaviors of the TEM waves have been described in many monographs on RF electrodynamics, for example in Refs. 64–66. According to their definition, the TEM waves have only transverse components of electric and magnetic fields and propagate at the velocity of light in medium (vacuum in the case of the 4CSTL).

In the case of TEM waves, a uniform wave equation which describes propagating characteristics of waveguide systems is reduced to the two-dimensional Laplace equation. As a result, the transverse fields of TEM waves are obtained from two-dimensional static equations and their longitudinal distributions are described by the telegraph equations. Thus, all the static field techniques are at our disposal in treatment of TEM waves. Because the transverse electric and magnetic fields are perpendicular between each other at everywhere and the ratio of their amplitudes is equal to the intrinsic impedance of free space $\sqrt{\mu_0/\epsilon_0}$, they are interconnected and each of them can be defined through each other. Hence, only the electrostatic problem is enough to be solved.

The propagation of TEM waves is described by the well-known telegraph equations[64-69]. The point by point derivation of them for the multi-conductor transmission line is presented, for example, in Ref. 66. For our case these equations can be derived from the consideration of the

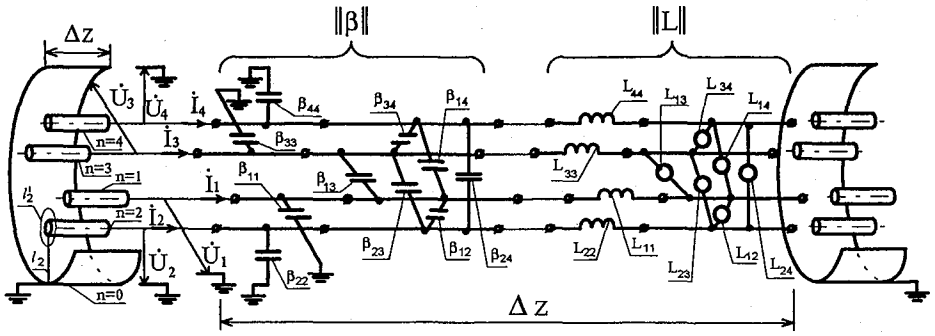

Fig. 4. Schematic representation for the distributed parameters of the 4CSTL.

elementary section of the 4CSTL with the length Δz, which are shown in figure 4 together with its equivalent circuit. The telegraph equations are formulated for the complex amplitudes of voltage and current on the conductors of the 4CSTL. These amplitudes are expressed as the integrals of the TEM wave fields. They depend on only the longitudinal coordinate z. For the n-th conductor (the shield corresponds to $n=0$) the integrals are taken along the some paths l_n and l_n', which are located in a transverse plane of the 4CSTL:

$$\dot{U}_n=-\int_{l_n}\dot{\vec{E}}\cdot d\vec{l}\ ,\quad \dot{I}_n=\oint_{l_n'}\dot{\vec{H}}\cdot d\vec{l} \tag{1}$$

The examples of these paths l_2 and l_2' for 2-nd conductor are shown in Fig. 4. Maxwell's equations are reduced to the system of the differential equations with $\dot{U}_n$ and $\dot{I}_n$ as the functions of z. This system is usually called as the telegraph equations. It consists of 2N differential equations for N-conductor transmission line, while the shield is the $(N+1)$-th conductor. For example, the simplest case of $N=1$ with 2 equations corresponds to the coaxial transmission line. The case of $N=4$ with 8 equations corresponds to the four-conductor shielded transmission line. For the 4CSTL this system can be written in the following matrix form:

$$\frac{d}{dz}\|\dot{\boldsymbol{U}}\|=-i\omega\cdot\|\boldsymbol{L}\|\cdot\|\dot{\boldsymbol{I}}\|,\quad \frac{d}{dz}\|\dot{\boldsymbol{I}}\|=-i\omega\cdot\|\beta\|\cdot\|\dot{\boldsymbol{U}}\|, \tag{2}$$

where $\|\boldsymbol{L}\|=\begin{bmatrix}L_{11}&L_{12}&L_{13}&L_{14}\\L_{21}&L_{22}&L_{23}&L_{24}\\L_{31}&L_{32}&L_{33}&L_{34}\\L_{41}&L_{42}&L_{43}&L_{44}\end{bmatrix}$, $\|\beta\|=\begin{bmatrix}\beta_{11}&\beta_{12}&\beta_{13}&\beta_{14}\\\beta_{21}&\beta_{22}&\beta_{23}&\beta_{24}\\\beta_{31}&\beta_{32}&\beta_{33}&\beta_{34}\\\beta_{41}&\beta_{42}&\beta_{43}&\beta_{44}\end{bmatrix}$, $\begin{cases}\beta_{ik}=\beta_{ki}\\ \\L_{ik}=L_{ki}\end{cases}$ for $i\neq k$,

$\|\dot{\boldsymbol{U}}\|=[\dot{U}_1,\dots,\dot{U}_4]^T$ and $\|\dot{\boldsymbol{I}}\|=[\dot{I}_1,\dots,\dot{I}_4]^T$ are 4-dimensional vectors of voltage and current, respectively; ω- is the angular frequency; $i^2=-1$. The sign T designates a transpose matrix. The matrices $\|\beta\|$ and $\|\boldsymbol{L}\|$ are 4×4-dimensional real square symmetric matrices. Their elements are the coefficients of the electrostatic induction and magnetostatic inductivity, respectively. The total definition of these coefficients is presented in Ref. 70–73. They can be obtained from corresponding electrostatic and magnetostatic problems for systems of N conductors.

The matrix $\|\beta\|$ expresses the total charges on the conductors $Q_1, Q_2, \dots, Q_N=\|\boldsymbol{Q}\|$ in terms of their potentials $\phi_1, \phi_2, \dots, \phi_N=\|\phi\|$, i.e.

$$\|\boldsymbol{Q}\|=\|\beta\|\cdot\|\phi\|. \tag{3}$$

While the coefficients of like index, as β_{ii}, are known as coefficients of capacity[70] (capacitance or the self-capacitance in Ref. 71) and of unlike index as coefficients of induction or the mutual capacitance. The β_{kk} are always positive ($\beta_{kk}>0$), but β_{ii} are negative ($\beta_{ik}=\beta_{ki}<0$).

The matrix $\|\boldsymbol{L}\|$ expresses the magnetic fluxes surrounding the conductors $\phi_1, \phi_2, \dots, \phi_N$ in terms of their currents $I_1, I_2, \dots, I_N$, i.e

$$\|\boldsymbol{\Phi}\|=\|\boldsymbol{L}\|\cdot\|\boldsymbol{I}\|. \tag{4}$$

The coefficients of like index, as L_{ii}, are known as the self-inductance and the coefficients of unlike index L_{ik} as the mutual inductance.

In this paper we consider only the symmetric four-conductor shielded transmission lines. Because these transmission lines have four conductors, their cross-sections have the rotational

symmetry for 90°. It means the followings : 1) all four conductors have identical cross-sections ; 2) the cross-section of the shield has the rotational symmetry for 90° (for example, a circle, a square, an octagon and so on) ; 3) conductors are located symmetrically relative to the center of symmetry of the shield. Then, there are the following additional relations between matrix coefficients for the symmetric 4CSTL, which are graphically illustrated by equivalent circuit of the 4CSTL in figure 4 :

$$\begin{aligned} &\beta_{11}=\beta_{22}=\beta_{33}=\beta_{44}\equiv\beta_a, \quad L_{11}=L_{22}=L_{33}=L_{44}\equiv L_a,\\ &\beta_{12}=\beta_{23}=\beta_{34}=\beta_{14}\equiv\beta_b, \quad L_{12}=L_{23}=L_{34}=L_{14}\equiv L_b,\\ &\beta_{13}=\beta_{24}\equiv\beta_c, \qquad\qquad L_{13}=L_{24}\equiv L_c \end{aligned} \tag{5}$$

The substitution of (5) into the telegraph equations (2) transfers them to the next form :

$$\frac{d}{dz}\begin{bmatrix}\dot U_1\\ \dot U_2\\ \dot U_3\\ \dot U_4\end{bmatrix}=-i\omega\cdot\begin{bmatrix}L_a & L_b & L_c & L_b\\ L_b & L_a & L_b & L_c\\ L_c & L_b & L_a & L_b\\ L_b & L_c & L_b & L_a\end{bmatrix}\cdot\begin{bmatrix}\dot I_1\\ \dot I_2\\ \dot I_3\\ \dot I_4\end{bmatrix},\quad \frac{d}{dz}\begin{bmatrix}\dot I_1\\ \dot I_2\\ \dot I_3\\ \dot I_4\end{bmatrix}=-i\omega\cdot\begin{bmatrix}\beta_a & \beta_b & \beta_c & \beta_b\\ \beta_b & \beta_a & \beta_b & \beta_c\\ \beta_c & \beta_b & \beta_a & \beta_b\\ \beta_b & \beta_c & \beta_b & \beta_a\end{bmatrix}\cdot\begin{bmatrix}\dot U_1\\ \dot U_2\\ \dot U_3\\ \dot U_4\end{bmatrix} \tag{6}$$

The common solution of system (6) for voltage and current can be expressed in terms of their boundary values at $z=0$. It consists of two waves traveling in opposite directions and can be written in the following matrix form (see for example, [69]):

$$\begin{aligned} \|\dot{\boldsymbol U}\| &= \exp(-\|\boldsymbol G\|\cdot z)\cdot\|\dot{\boldsymbol U}^{(+)}_{z=0}\| + \exp(\|\boldsymbol G\|\cdot z)\cdot\|\dot{\boldsymbol U}^{(-)}_{z=0}\| ;\\ \|\dot{\boldsymbol I}\| &= \exp(-\|\boldsymbol G\|^T\cdot z)\cdot\|\dot{\boldsymbol I}^{(+)}_{z=0}\| + \exp(\|\boldsymbol G\|^T\cdot z)\cdot\|\dot{\boldsymbol I}^{(-)}_{z=0}\| ; \end{aligned} \tag{7}$$

where- $\|\boldsymbol G\|=\sqrt{\|\boldsymbol L\|\cdot\|\beta\|}$ is a square symmetric matrix. Their elements are the coefficients of propagation and $\|\boldsymbol G\|^T=\sqrt{\|\beta\|\cdot\|\boldsymbol L\|}$. The plus sign designates a forward wave and the minus corresponds to backward one.

This solution of the telegraph equations describes the longitudinal distributions of voltage and current and they correspond to the electric and magnetic fields of the TEM waves. The transverse pictures of these fields are defined by two-dimensional (2D) Laplace equations with boundary conditions determined by the voltage and current values at a given cross-section. As it is followed from above expressions, the voltage and current on every conductor of the transmission line depend on the voltage and current on the rest conductors. In general case, it means that the ratios of voltage and current between conductors change along the 4CSTL and the boundary conditions at every cross-sections will be different. Consequently, the 2D-problems also will be different for each cross-section and the transverse pictures of the TEM waves will depend on longitudinal position along transmission line. In such case it is necessary to solve Laplace equations for every cross-section and further procedures will become a numerical one. This causes difficulties for qualitative interpretations.

4. NORMAL MODES OF THE 4CSTL

4.1 *Mathematical derivation*

In order to eliminate the difficulties coming from the longitudinal dependence of 2-D problems we use the normal mode analysis technique for TL. Originally, this method was developed for the high-voltage multi-conductor transmission lines[64-69]. In a particular case of

the 2-conductor transmission lines this procedure are widely applied to study RF devices working on two coupled transmission lines (directional couplers, filters, amplifiers, slow-waves transmission systems and so on). The simplest variant of normal mode technique for two coupled lines was also adapted to study the 4-rod RFQ at the assumption in which two opposite electrodes are treated as a single conductor[4,7,49,50,60,61,63,74]. Because the 4CSTL corresponds to the 4-rod RFQ more adequately, we have extended this method to the 4CSTL. This makes it possible to generalize the consideration for the 4-rod RFQ. In the previous papers[49,50,63] we have already presented such extension shortly. In this paper we describe the normal mode analysis technique developed for the 4CSTL in detail.

The normal mode technique introduces a concept of so-called normal TEM waves (or modes), which are also characterized by some voltage $\|\dot{\xi}\|$ and current $\|\dot{\eta}\|$. The voltage and current of these normal modes are some combinations of voltage $\|\dot{U}\|$ and current $\|\dot{I}\|$ of original TEM waves. In a transmission line system with N conductors there are N normal TEM modes of propagation. Thus, there are four modes in the 4CSTL. Any field of original TEM waves is expressed by the superposition of these normal modes.

Mathematically, the problem of a definition of normal modes corresponds to the calculation of the so-called modal matrix $\|\boldsymbol{M}\|$[64,66], which converts the square matrices $\|\beta\|$ and $\|\boldsymbol{L}\|$ of the initial system (4) into the diagonal form. The modal matrix $\|\boldsymbol{M}\|$ is composed of eigenvectors (or modal column) $\|\boldsymbol{V}\|$ of conversed matrixes which correspond to their eigenvalues (or characteristic roots). Let ζ_β designates the eigenvalue of $\|\beta\|$ and ζ_L of $\|\boldsymbol{L}\|$. Due to the matrices $\|\beta\|$ and $\|\boldsymbol{L}\|$ are the commutative ones, i.e. $\|\beta\|\cdot\|\boldsymbol{L}\|=\|\boldsymbol{L}\|\cdot\|\beta\|$, they have the same eigenvectors and modal matrix $\|\boldsymbol{M}\|$. The eigenvectors $\|\boldsymbol{V}\|$ satisfy to the both following equations:

$$\|\boldsymbol{L}\|\cdot\|\boldsymbol{V}\|=\zeta_L\cdot\|\boldsymbol{V}\|, \quad \|\beta\|\cdot\|\boldsymbol{V}\|=\zeta_\beta\cdot\|\boldsymbol{V}\| \tag{8}$$

The characteristic roots are derived from characteristic equations for matrices $\|\beta\|$ and $\|\boldsymbol{L}\|$:

$$\det(\|\boldsymbol{L}\|-\zeta_L\cdot\|\boldsymbol{V}\|)=0, \quad \det(\|\beta\|-\zeta_\beta\cdot\|\boldsymbol{E}\|)=0, \tag{9}$$

where $\|\boldsymbol{E}\|$ is the unit matrix. Both these equations result in the similar fourth order algebraic equations with respect to the characteristic roots. Their decisions are expressed as the followings:

$$\begin{cases}\zeta_{L1}=L_a+2L_b+L_c;\ \zeta_{L2}=L_a-2L_b+L_c;\ \zeta_{L3}=L_a-L_c;\ \zeta_{L4}=L_a-L_c\\ \zeta_{\beta1}=\beta_a+2\beta_b+\beta_c;\ \zeta_{\beta2}=\beta_a-2\beta_b+\beta_c;\ \zeta_{\beta3}=\beta_a-\beta_c;\ \zeta_{\beta4}=\beta_a-\beta_c\end{cases} \tag{10}$$

Substitution of these eigenvalues into the equations (8) defines the eigenvectors $\|\boldsymbol{V}\|$ and, hence, the modal matrix $\|\boldsymbol{M}\|$:

$$\|\boldsymbol{M}\|=\frac{1}{2}\cdot\begin{bmatrix}1 & 1 & 1 & 1\\ 1 & -1 & 1 & -1\\ 1 & 1 & -1 & -1\\ 1 & -1 & -1 & 1\end{bmatrix}. \tag{11}$$

As $\|\boldsymbol{M}\|$ is a symmetric matrix, it satisfies to the following relations:

$$\|\boldsymbol{M}\|^T=\|\boldsymbol{M}\|^{-1}=\|\boldsymbol{M}\|, \quad \|\boldsymbol{M}\|\cdot\|\boldsymbol{M}\|^T=\|\boldsymbol{M}\|\cdot\|\boldsymbol{M}\|^{-1}=\|\boldsymbol{E}\| \tag{12}$$

Besides the matrix $\|\boldsymbol{M}\|$, the normalized matrix $\|\boldsymbol{D}\|$ [69] should be defined for convenience of physical interpretation of the normal modes. We have defined it in the following form:

$$\|\boldsymbol{D}\|=\begin{bmatrix}1/2 & 0 & 0 & 0\\ 0 & 1 & 0 & 0\\ 0 & 0 & 1 & 0\\ 0 & 0 & 0 & 1\end{bmatrix},\quad \|\boldsymbol{D}\|^{-1}=\begin{bmatrix}2 & 0 & 0 & 0\\ 0 & 1 & 0 & 0\\ 0 & 0 & 1 & 0\\ 0 & 0 & 0 & 1\end{bmatrix}\quad (\|\boldsymbol{D}\|\cdot\|\boldsymbol{D}\|^{-1}=\|\boldsymbol{E}\|) \tag{13}$$

In order to transfer from the telegraph equations for original TEM waves (6) to ones for the normal modes we should follow to the methodology in Refs. 66, 69. Let's insert into right-hand sides of equations (6) the factors $\|\boldsymbol{M}\|\cdot\|\boldsymbol{M}\|^{T}=\|\boldsymbol{E}\|$ and $\|\boldsymbol{D}\|\cdot\|\boldsymbol{D}\|^{-1}=\|\boldsymbol{E}\|$ one after other:

$$\frac{d}{dz}\|\dot{\boldsymbol{U}}\|=-i\omega\cdot\|\boldsymbol{L}\|\cdot\|\boldsymbol{M}\|\cdot\|\boldsymbol{D}\|\cdot\|\boldsymbol{D}\|^{-1}\cdot\|\boldsymbol{M}\|^{T}\cdot\|\dot{\boldsymbol{I}}\|,$$

$$\frac{d}{dz}\|\dot{\boldsymbol{I}}\|=-i\omega\cdot\|\beta\|\cdot\|\boldsymbol{M}\|\cdot\|\boldsymbol{D}\|^{-1}\cdot\|\boldsymbol{D}\|\cdot\|\boldsymbol{M}\|^{T}\cdot\|\dot{\boldsymbol{U}}\|$$

Then, multiply both sides of the voltage equation by factor $\|\boldsymbol{D}\|\cdot\|\boldsymbol{M}\|^{T}$ and the current equation by factor $\|\boldsymbol{D}\|^{-1}\cdot\|\boldsymbol{M}\|^{T}$:

$$\begin{aligned}&\frac{d}{dz}\|\boldsymbol{D}\|\cdot\|\boldsymbol{M}\|^{T}\cdot\|\dot{\boldsymbol{U}}\|=-i\omega\cdot\|\boldsymbol{D}\|\cdot\|\boldsymbol{M}\|^{T}\cdot\|\boldsymbol{L}\|\cdot\|\boldsymbol{D}\|\cdot\|\boldsymbol{D}\|^{-1}\cdot\|\boldsymbol{M}\|^{T}\cdot\|\dot{\boldsymbol{I}}\|,\\ &\frac{d}{dz}\|\boldsymbol{D}\|^{-1}\cdot\|\boldsymbol{M}\|^{T}\cdot\|\dot{\boldsymbol{I}}\|=-i\omega\cdot\|\boldsymbol{D}\|^{-1}\cdot\|\boldsymbol{M}\|^{T}\cdot\|\beta\|\cdot\|\boldsymbol{M}\|\cdot\|\boldsymbol{D}\|^{-1}\cdot\|\boldsymbol{D}\|\cdot\|\boldsymbol{M}\|^{T}\cdot\|\dot{\boldsymbol{U}}\|\end{aligned} \tag{14}$$

The equations (14) can be written in the short form:

$$\frac{d}{dz}\|\dot{\xi}\|=-i\omega\cdot\|\boldsymbol{L}^{D}\|\cdot\|\dot{\eta}\|,\quad \frac{d}{dz}\|\dot{\eta}\|=-i\omega\cdot\|\beta^{D}\|\cdot\|\dot{\xi}\|, \tag{15}$$

where $\|\dot{\xi}\|=\|\boldsymbol{D}\|\cdot\|\boldsymbol{M}\|^{T}\cdot\|\dot{\boldsymbol{U}}\|,\quad \|\dot{\eta}\|=\|\boldsymbol{D}\|^{-1}\cdot\|\boldsymbol{M}\|^{T}\cdot\|\dot{\boldsymbol{I}}\|,$

$$\|\boldsymbol{L}^{D}\|=\|\boldsymbol{D}\|\cdot\|\boldsymbol{M}\|^{T}\cdot\|\boldsymbol{L}\|\cdot\|\boldsymbol{M}\|\cdot\|\boldsymbol{D}\|=\begin{bmatrix}\zeta_{L1}/4 & 0 & 0 & 0\\ 0 & \xi_{L2} & 0 & 0\\ 0 & 0 & \xi_{L3} & 0\\ 0 & 0 & 0 & \xi_{L4}\end{bmatrix},$$

$$\|\beta^{D}\|=\|\boldsymbol{D}\|^{-1}\cdot\|\boldsymbol{M}\|^{T}\cdot\|\beta\|\cdot\|\boldsymbol{M}\|\cdot\|\boldsymbol{D}\|^{-1}=\begin{bmatrix}4\zeta_{\beta1} & 0 & 0 & 0\\ 0 & \zeta_{\beta2} & 0 & 0\\ 0 & 0 & \zeta_{\beta3} & 0\\ 0 & 0 & 0 & \zeta_{\beta4}\end{bmatrix}$$

and the elements $\zeta_{L1},\dots,\zeta_{L4}$ and $\zeta_{\beta1},\dots,\zeta_{\beta4}$ are defined by formulae (10).

As the result, the system of telegraph equations (6) consisting of 8 $(2\times N)$ coupled equations is reduced to four independent systems. Each of these systems contains the two simplest telegraph equations for each normal mode:

$$\overbrace{\begin{cases}\frac{d}{dz}\dot{\xi}_1=-i\omega\cdot L_{11}^{D}\cdot\dot{\eta}_1\\ \frac{d}{dz}\dot{\eta}_1=-i\omega\cdot\beta_{11}^{D}\cdot\dot{\xi}_1\end{cases}}^{\text{1-st mode:}},\qquad \overbrace{\begin{cases}\frac{d}{dz}\dot{\xi}_2=-i\omega\cdot L_{22}^{D}\cdot\dot{\eta}_2\\ \frac{d}{dz}\dot{\eta}_2=-i\omega\cdot\beta_{22}^{D}\cdot\dot{\xi}_2\end{cases}}^{\text{2-th mode:}},$$

$$\overbrace{\begin{cases}\frac{d}{dz}\dot{\xi}_3=-i\omega\cdot L_{33}^{D}\cdot\dot{\eta}_3\\ \frac{d}{dz}\dot{\eta}_3=-i\omega\cdot\beta_{33}^{D}\cdot\dot{\xi}_3\end{cases}}^{\text{3-th mode:}},\quad \overbrace{\begin{cases}\frac{d}{dz}\dot{\xi}_4=-i\omega\cdot L_{44}^{D}\cdot\dot{\eta}_4\\ \frac{d}{dz}\dot{\eta}_4=-i\omega\cdot\beta_{44}^{D}\cdot\dot{\xi}_4\end{cases}}^{\text{4-th mode:}}, \tag{16}$$

Each of four systems given by (16) can be solved as a usual telegraph equation for one-conductor (or coaxial) transmission line. From (16) the second order differential equations describing the voltage wave propagation of every normal wave can be derived:

$$\frac{d^2}{dz^2}\dot{\xi}_i=-\gamma_i^2\cdot\dot{\xi}_i,\ i=1,\dots,4,\quad \text{where-}\ \gamma_i=\omega^2\cdot L_{ii}^{D}\cdot\beta_{ii}^{D} \tag{17}$$

Taking into account that the TEM waves propagate at the velocity of light ν, all constants of propagation γ_i should be the same and be equal to the wave number $k=\omega/\nu$, i.e. $\gamma_i\equiv k$. This means that coefficients L_{ii}^{D} and β_{ii}^{D} are interconnected by the relation

$$L_{ii}^{D}\cdot\beta_{ii}^{D}=\frac{1}{\nu^2}. \tag{18}$$

Using this relation the solution for normal modes is expressed in the matrix form as:

$$\begin{aligned}\|\dot{\xi}\|&=\|\dot{\boldsymbol{A}}\|\cdot\cos(kz)+\|\dot{\boldsymbol{B}}\|\cdot\sin(kz),\\ \|\dot{\eta}\|&=i\cdot\nu\cdot\|\beta^{D}\|\cdot\{-\|\dot{\boldsymbol{A}}\|\cdot\sin(kz)+\|\dot{\boldsymbol{B}}\|\cdot\cos(kz)\},\end{aligned} \tag{19}$$

$\|\dot{\boldsymbol{A}}\|$ and $\|\dot{\boldsymbol{B}}\|$ are vectors of constant coefficients defined by boundary conditions.

Finally, the solution for the full field of the 4CSTL can be obtained from the results for normal modes (19). The expressions for voltage and current of an original TEM wave through the normal modes can be derived from relations (15) in the following form:

$$\begin{aligned}\|\dot{\boldsymbol{U}}\|&=\|\boldsymbol{M}\|\cdot\|\boldsymbol{D}\|^{-1}\cdot\|\dot{\xi}\|=\frac{1}{2}\cdot\begin{bmatrix}2&1&1&1\\2&-1&1&-1\\2&1&-1&-1\\2&-1&-1&1\end{bmatrix}\cdot\|\dot{\xi}\|,\\ \|\dot{\boldsymbol{I}}\|&=\|\boldsymbol{M}\|\cdot\|\boldsymbol{D}\|\cdot\|\dot{\eta}\|=\frac{1}{2}\cdot\begin{bmatrix}1/2&1&1&1\\1/2&-1&1&-1\\1/2&1&-1&-1\\1/2&-1&-1&1\end{bmatrix}\cdot\|\dot{\eta}\|\end{aligned} \tag{20}$$

4.2 *Physical interpretations of TEM modes*

Let's consider the meanings of introduced normal mode parameters. The relations (15) for normal mode voltage and currents are

$$\begin{aligned}\dot{\xi}_1&=1/4\cdot(\dot{U}_1+\dot{U}_2+\dot{U}_3+\dot{U}_4) & \dot{\eta}_1&=(\dot{I}_1+\dot{I}_2+\dot{I}_3+\dot{I}_4)\\ \dot{\xi}_2&=1/2\cdot(\dot{U}_1-\dot{U}_2+\dot{U}_3-\dot{U}_4) & \dot{\eta}_2&=1/2\cdot(\dot{I}_1-\dot{I}_2+\dot{I}_3-\dot{I}_4)\\ \dot{\xi}_3&=1/2\cdot(\dot{U}_1+\dot{U}_2-\dot{U}_3-\dot{U}_4) & \dot{\eta}_3&=1/2\cdot(\dot{I}_1+\dot{I}_2-\dot{I}_3-\dot{I}_4)\\ \dot{\xi}_5&=1/2\cdot(\dot{U}_1-\dot{U}_2-\dot{U}_3+\dot{U}_4) & \dot{\eta}_4&=1/2\cdot(\dot{I}_1-\dot{I}_2-\dot{I}_3+\dot{I}_4)\end{aligned} \tag{21}$$

To obtain the conditions for existence of only a single mode, we should put voltage and currents of any others to be equal zero. For example, for the first mode it means that $\dot{\xi}_2\equiv\dot{\xi}_3\equiv\dot{\xi}_4\equiv 0$ and $\dot{\eta}_2\equiv\dot{\eta}_3\equiv\dot{\eta}_4\equiv 0$ at any z. Their substitution in (21) will give that voltage and current

of TEM wave are identical on all conductors, i.e $\dot{U}_1 \equiv \dot{U}_2 \equiv \dot{U}_3 \equiv \dot{U}_4 \equiv \dot{U}$ and $\dot{I}_1 \equiv \dot{I}_2 \equiv \dot{I}_3 \equiv \dot{I}_4 \equiv \dot{I}$. The voltage and current of the first normal mode are $\dot{\xi}_1 \equiv \dot{U}$ and $\dot{\eta}_2 \equiv 4 \cdot \dot{I}$. The similar procedure can be applied for other modes. The voltage and current of normal modes in the absence of any other mode components are connected with the voltage and current of original TEM waves in the following way:

$$\begin{cases} \dot{\xi}_1 = \dot{U},\ \dot{U} \equiv \dot{U}_1 \equiv \dot{U}_2 \equiv \dot{U}_3 \equiv \dot{U}_4 \\ \dot{\eta}_1 = 4 \cdot \dot{I},\ \dot{I} \equiv \dot{I}_1 \equiv \dot{I}_2 \equiv \dot{I}_3 \equiv \dot{I}_4 \end{cases}, \quad \begin{cases} \dot{\xi}_2 = 2 \cdot \dot{U},\ \dot{U} \equiv \dot{U}_1 \equiv -\dot{U}_2 \equiv \dot{U}_3 \equiv -\dot{U}_4 \\ \dot{\eta}_2 = 2 \cdot \dot{I},\ \dot{I} \equiv \dot{I}_1 \equiv -\dot{I}_2 \equiv \dot{I}_3 \equiv -\dot{I}_4 \end{cases},$$

$$\begin{cases} \dot{\xi}_3 = 2 \cdot \dot{U},\ \dot{U} \equiv \dot{U}_1 \equiv \dot{U}_2 \equiv -\dot{U}_3 \equiv -\dot{U}_4 \\ \dot{\eta}_3 = 2 \cdot \dot{I},\ \dot{I} \equiv \dot{I}_1 \equiv \dot{I}_2 \equiv -\dot{I}_3 \equiv -\dot{I}_4 \end{cases}, \quad \begin{cases} \dot{\xi}_4 = 2 \cdot \dot{U},\ \dot{U} \equiv \dot{U}_1 \equiv -\dot{U}_2 \equiv -\dot{U}_3 \equiv \dot{U}_4 \\ \dot{\eta}_4 = 2 \cdot I,\ \dot{I} \equiv \dot{I}_1 \equiv -\dot{I}_2 \equiv -\dot{I}_3 \equiv \dot{I}_4 \end{cases} \qquad (22)$$

From these relations, we may define the ways of connections of the conductors of the 4CSTL for each mode under the condition that any other mode components are absent. Every mode propagates along all conductors of TL making up the so-called modal channel. The top row of figure 5 illustrates the modal channels of the 4CSTL graphically. Every modal channel of the 4CSTL can be considered as simple transmission line system with two conductors, one of them with a direct current and other with a reversed one.

The mathematically derived relations (22) express the practically important fact that the ratio between voltage and current on the conductors for every mode do not change along TL. It allows to use for every mode the same mathematical means as the usual one-conductor TL (for example, coaxial or non-shielded two-conductor TL). That is, in order to determine the TEM fields, it is necessary to carry out two procedures for every mode. First one is calculation of

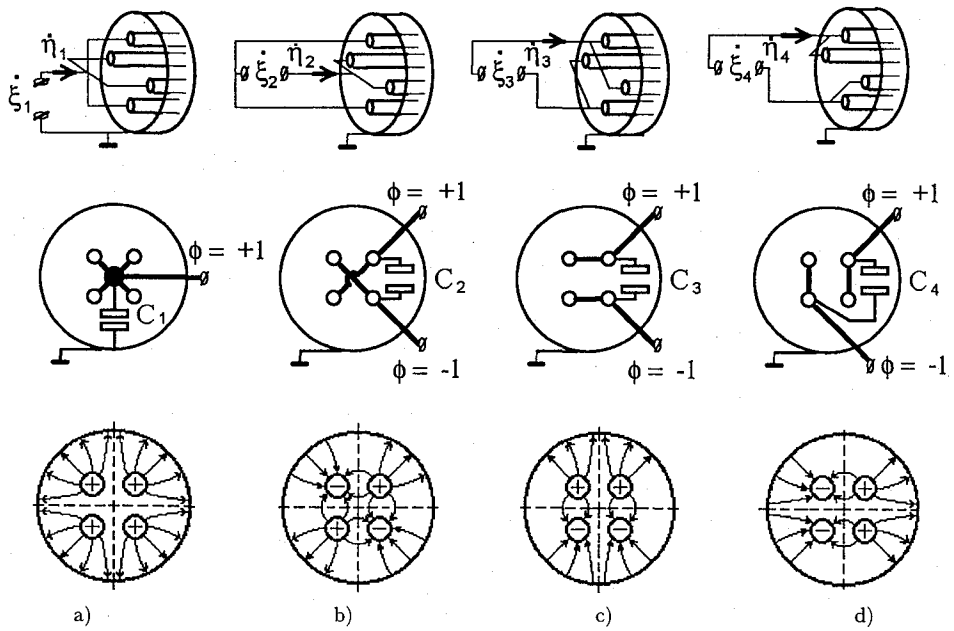

Fig. 5. Normal TEM modes in the 4CSTL. The 1st, 2nd, 3rd and 4th modes correspond to figures a), b), c) and d), respectively. The top row is the "modal channels" of the 4CSTL, the middle is the 2-D problems for definition of distributed capacitance, the bottom is the E-line patterns.

distributed parameters. They are derived from the 2-D problems, which correspond to every mode channel. The second step is the determination of longitudinal dependence which is derived from the solutions of the corresponding telegraph equations (16).

The every modal channel of the 4CSTL shown in the top row of figure 5 is characterized by the distributed capacitance C_i and inductance L_i. The two-dimensional electrostatic problems with definition of capacitance C_i are presented in the middle row of figure 5. These distributed parameters C_i and L_i are equal to the corresponding diagonal elements of matrices $\|\beta^D\|$ and $\|\boldsymbol{L}^D\|$, respectively:

$$\begin{cases} C_1=\beta_{11}^D=4\zeta_{\beta 1}=4(\beta_a+2\beta_b+\beta_c) \\ C_2=\beta_{22}^D=\zeta_{\beta 2}=\beta_a-2\beta_b+\beta_c \\ C_3=\beta_{33}^D=\zeta_{\beta 3}=\beta_a-\beta_c \\ C_4=\beta_{44}^D=\zeta_{\beta 4}=\beta_a-\beta_c \end{cases} ; \quad \begin{cases} L_1=L_{11}^D=\dfrac{\zeta_{L1}}{4}=\dfrac{1}{4}\cdot(L_a+2L_b+L_c) \\ L_2=L_{22}^D=\zeta_{L2}=L_a-2L_b+L_c \\ L_3=L_{33}^D=\zeta_{L3}=L_a-L_c \\ L_4=L_{44}^D=\zeta_{L4}=L_a-L_c \end{cases} \tag{23}$$

Using the formulae (3) and (4) it is easy to check these relations (23). The capacitance C_1 is defined to be a capacitor. The first terminal of this capacitor corresponds to the four central conductors of the 4CSTL connected together. The second terminal correspond to the shield of the 4CSTL. The capacity is the ratio of the charge Q on one terminal to the potential difference U of between them. The charge Q is the sum of the four equal charges Q_1 of four conductors of the 4CSTL, i.e. $Q=4\cdot Q_1$, while they have the same potential U. Using (3) the charge on the one central conductor Q_1 is expressed as $Q_1=(\beta_a+2\beta_b+\beta_c)\cdot U$. Hence, the capacitance C_1 becomes $C_1=4\cdot(\beta_a+2\beta_b+\beta_c)$.

The inductance L_1 is defined as an inductivity of a single conductor. This conductor corresponds to the four central conductors of the 4CSTL connected together surrounded by the shield of the 4CSTL. The inductivity is the ratio of the flux Φ surrounding this conductor to its current I. This current I is the sum of the four equal currents I_1 of four conductors of the 4CSTL, i.e. $I=4\cdot I_1$, while they are surrounded by the same magnetic fluxes Φ. Using (4) the magnetic fluxes Φ surrounding any central conductor is expressed as $\Phi=(L_a+2L_b+L_c)\cdot I/4$. Hence, the inductance L_1 becomes $L_1=(L_a+2L_b+L_c)/4$.

The similar considerations may be carried out for other modes. Because of the interconnection of the electric and magnetic fields, there is the relation (18), which couples the distributed capacitance C_i and the distributed inductance L_i. This means that it is enough to calculate only the distributed capacitance C_i. The distributed inductance L_i can be obtained by the relation (18).

The bottom row of Figure 5 illustrates the E-line patterns of normal TEM modes in the 4CSTL. It shows clear the physical meaning of each mode. The first mode can be named as the coaxial, because it corresponds to the usual CTL with four-wire central conductor. The second mode is a quadrupole one. It creates the original RFQ fields and therefore, their longitudinal distribution will determine the voltage flatness in RFQ-channel. The third and fourth modes are two dipole modes. The directions of their fields are perpendicular to each other.

If we accept the usual approximation that the current flowing on the real 4CSTL with losses are the same as in the ideal 4CSTL without losses, the total power loss P becomes the simple sum of the partial loss of every mode P_i, i.e. $P=\sum_{i=1}^{i=4} P_i$. Only the second mode has useful field for

RFQ. In view point of power loss the rest modes can be considered as "parasitic" ones.

However, the non-quadrupole modes may be responsible for some other properties of the resonator. For example, the presence of coaxial mode determine a very flat field of the "Alternate stems 4-rod RFQ" resonator with a small tank diameter. Moreover, these non-quadrupole modes also may contribute some additional corrections in beam dynamics.

Although the coaxial mode does not penetrate the accelerating channel, but it makes some potential difference between the axis of RFQ channel and the resonator tank. This fact should be taken into consideration for design of an matching sections. For example, it was shown in Ref. 8 for the SCR that the electrode shapes must be modified essentially. In the case of the SCR the existence of such potential difference is obvious even without the present normal mode concept. However, there are some constructions of 4-rod RFQ in Refs. 5, 9, 10, 13, where the existence of such voltage is not so clear. In these cases, using the normal mode analysis, we may detect the presence of coaxial mode which creates undesirable potential difference in a matching area. It can help to find the best ways for construction of a matching section of the 4-rod RFQ.

The simple constructive design of structure can be reached when the presence of the weak dipole fields is allowed[13,28,37,39]. In contrary of coaxial mode, the dipole modes may influence on beam dynamics in a regular part of RFQ channel. Their fields should be added to an original RFQ field, because they may cause both resonant and non-resonant interactions with particles of beams and therefore, can distort the stable particle motion. It is useful to know the conditions for existence of non-quadrupole modes in order to evaluate their affects or to find means to suppress them.

At first the normal mode analysis was introduced only to eliminate the mathematical difficulties. However, the practical importance of the normal modes has increased by the fact that the normal modes have clear physical interpretations. The knowledge of the mode contents of total field in the 4CSTL can be useful for calculations of both efficiencies of 4-rod RFQ resonators and the beam dynamics in their RFQ-channel.

5. THE PROPAGATING MODE CONTENTS OF CAVITY MODES

In the indefinite 4CSTL, the normal TEM modes can propagate with any amplitudes at any frequencies. But if the conductors of the 4CSTL will be loaded by some impedance, this system becomes a resonance circuit with several resonance modes at a discrete set of frequencies, while the TEM wave of each *resonance* mode is a superposition of the *propagating* normal TEM modes of the 4CSTL. The amplitudes of these field components depend on the configurations of resonators. A resonance mode of a 4-rod RFQ resonator can be described by a combination of the corresponding normal TEM modes. Such combination can distinguish a type of a resonator. Some cases of the mode combination in the 4CSTL and corresponding 4-rod RFQ resonators are discussed in the following sections. This approximate method is compared with field patterns obtained from the exact solution of Maxwell's equations which was made by us using the 3-D MAFIA code[75].

5.1 *4-rod resonators on the base of a single TEM propagating mode.*

At the beginning, the simplest case is considered when the cavity mode is formed by a single normal mode. Let's consider the standing waves produced by every normal mode. They can be excited in the corresponding modal channels of the 4CSTL presented in Fig. 5. They are

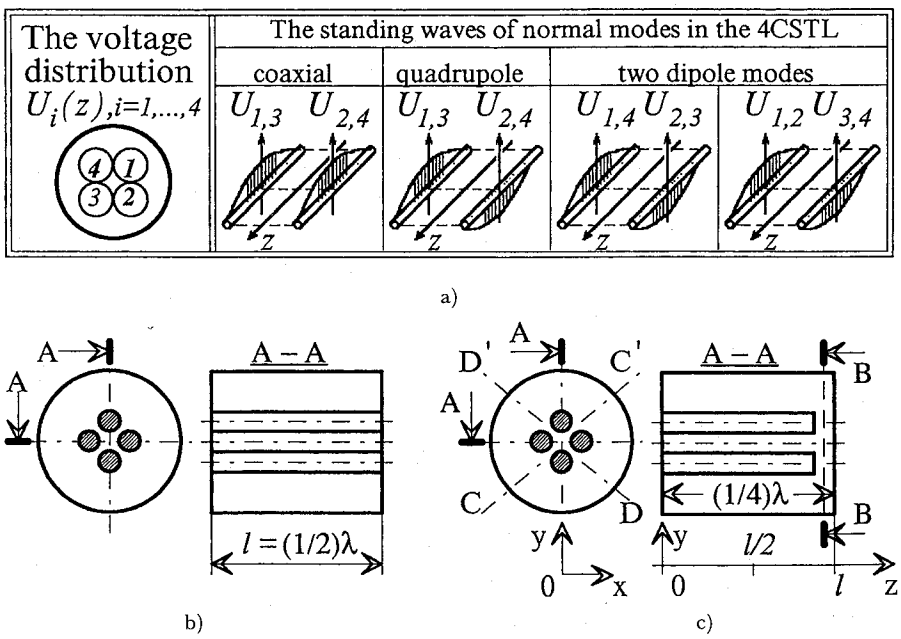

Fig. 6. a) the voltage distribution of the standing waves produced by every normal mode in the 4CSTL; b) half-wave 4-rod resonator; c) quarter-wavelength 4-rod RFQ resonator.

usual standing waves of a simple TL with voltage and current nodes shifted exactly by a quarter wavelength. Then, we cut the 4CSTL between two voltage nodes. The Fig. 6, a represents the voltage distribution in such section for every mode. This section becomes a resonance circuit, which corresponds to half-wave 4-rod resonator (Fig. 6, b). Note, this resonator is a single example where present method decides the 3-D electrodynamics problem exactly.

The half-wave 4-rod resonator has four main resonant modes and each of them is produced by a single normal propagating mode. Because they have the same resonance conditions expressed as $l=\lambda/2$, their resonant frequencies coincide. All cavity modes are confluent and we cannot see them separately on the field patterns produced by MAFIA code. This resonator has no practical interest. But cutting of it into two pieces makes the quarter-wavelength 4-rod RFQ resonator (Fig. 6, c). In this case, almost all modes are separated and their fields drawn by MAFIA-code are illustrated in fiigure 7.

The Fig. 7, a presents E-lines and B-lines of the cavity modes at the transverse cross-section of $\lambda/4$-resonator at $z=l/2$. These field patterns are in good agreement with the corresponding TEM propagating normal modes which were given already in Fig. 5. The transverse field patterns of resonator are the same almost at all values of z. The exception is only a narrow region near the open ends of electrodes at $z=l$, where the E-lines have dominant longitudinal components. The fields at transverse cross-section at $z=l$ are shown in Fig. 7, b. The fields of quadrupole cavity mode in axial planes of $\lambda/4$-resonator are given in Fig. 7, c. It illustrates that the fields have mainly transverse components.

It is seen that the fields have the transverse E and B components corresponding TEM waves and are distributed along z-axis in the same manner as fields of usual coaxial $\lambda/4$-resonator, the

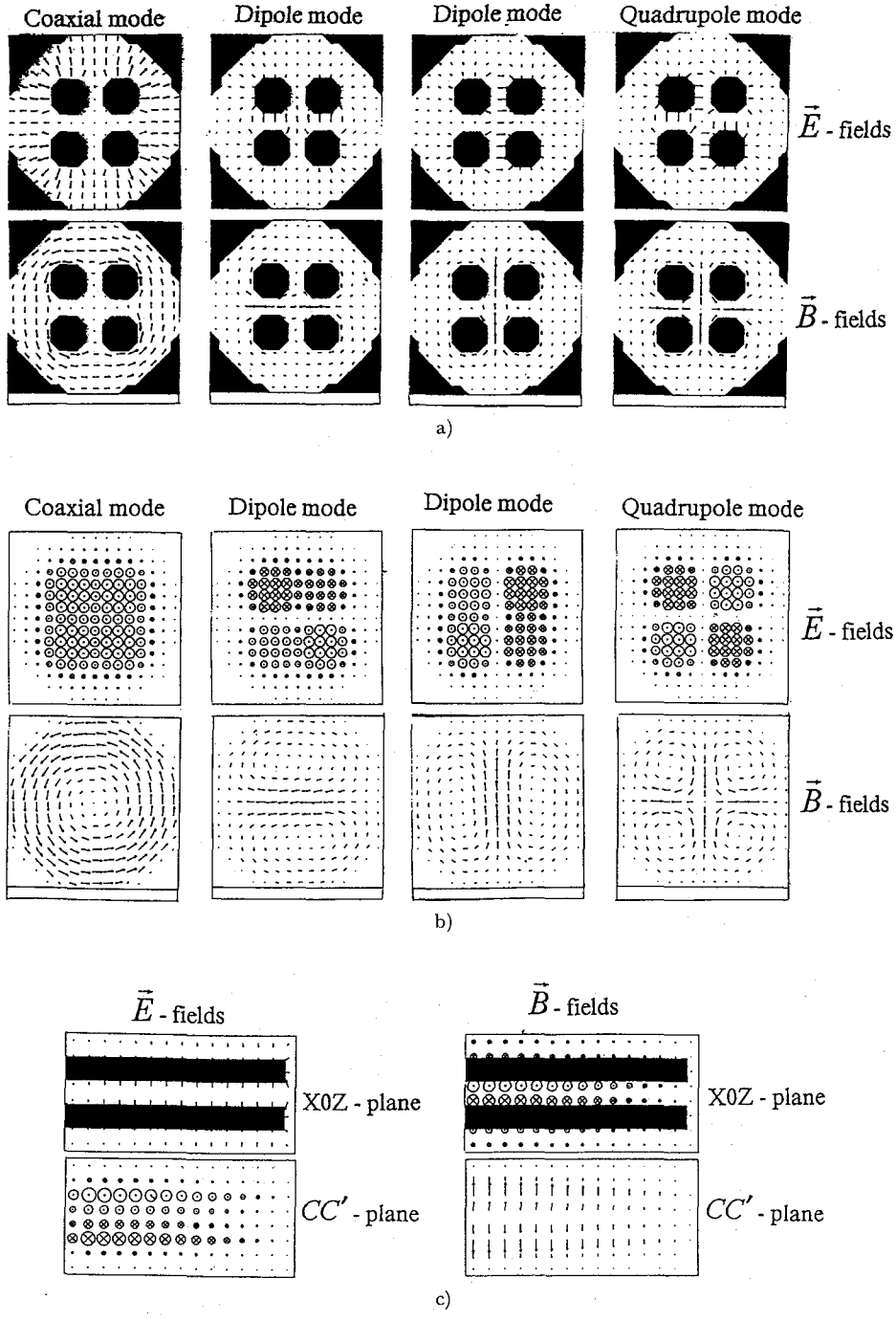

Fig. 7. The field patterns of the cavity modes calculated by MAFIA code for the of $\lambda/4$-resonator which is shown in Fig. 6, c: a) the fields in the transverse cross-section at $z=l/2$; b) the fields in the transverse cross-section at $z=l$; c) The fields of quadrupole cavity mode in axial planes X0Z and CC'.

one end of which is terminated by a short circuit and the other by loading capacity. Hence, the resonance conditions of this 4-rod $\lambda/4$-resonator are determined by the same way as the case of its coaxial analogue, namely $ctg(kl)=k\cdot C_i^l/C_i$, where Ci and C_i^l are the distributed capacitance (see Fig. 5) and loading capacities, respectively, for the i-th normal mode. The Fig. 7, c explains by example the difference of C_i^l for unlike modes. Under the influence of the loading capacity, the resonance frequencies of cavity modes are reduced from the resonant frequency $f_{\lambda/4}=c/4l$ of an ideal case where the loading is absent.

Thus, there is the mode separation for the case of $\lambda/4$-resonator in comparison with $\lambda/2$-resonator. It is predetermined by the different values of the ratios C_i^l/C_i. The mode separation can reach up to several percents for the reasonable geometry of resonators at the open end areas. For example, for $\lambda/4$-resonator presented in Fig. 6, c, where its length, the tank diameter, the electrode diameters and the gap width at open ends are 0.2 m, 0.1 m, 0.01 m and 0.01 m, respectively, the $f_{\lambda/4}$-value becomes to be 375 MHz. The calculated frequencies by MAFIA-code are 332 MHz (the difference from $f_{\lambda/4}$ is 11%), 366 MHz (2.5%) and 373 MHz (0.5%) for coaxial, dipole and quadrupole modes, respectively. The results show that quadrupole cavity mode is insensitive to the loading capacity.

Because of the sinusoidal change of the longitudinal voltage distribution, the quarupole fields of the given $\lambda/4$-resonator is essentially non-uniform along resonator axis. This is not practical without modification. The modification is similar to drift-tube structures of the Sloan-Lawrence type on twin-line. The non-uniformity of the voltage distribution is reduced by "bending the low voltage parts" [52-54]. The Fig. 8 shows the results of such modification of $\lambda/2$-resonator (Fig. 6, b) into one-section of 4-rod resonator. The generalization of the one-section makes the indefinite multi-sectional resonator. It is seen how the electrodes in "low voltage parts" of $\lambda/2$-resonator transform into the electrode-supporting posts of multi-sectional resonator. According to longitudinal positions of supporting posts, this resonator is called the 4-rod RFQ resonator with "In-line stems".

The "bending" procedure is mechanically looked as cutting of the low voltage parts of electrodes with the arrangement of the supporting posts at the cutting points. With equivalent circuits, it may be treated as a connection of some equivalent impedance of the supporting posts

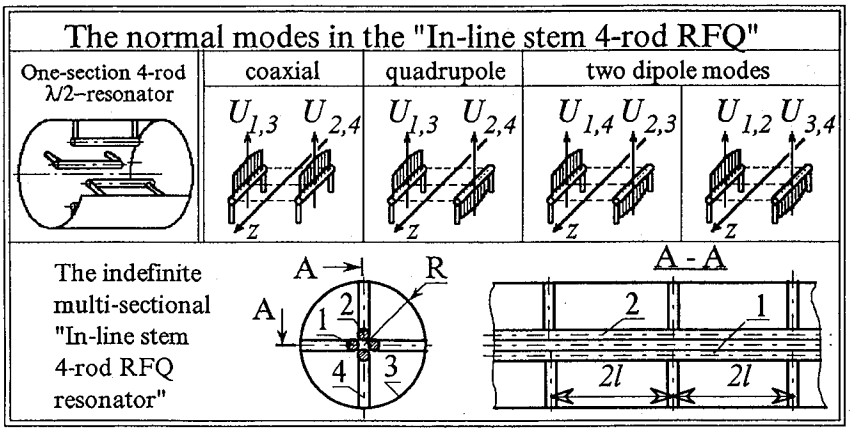

Fig. 8. The normal modes in the one section of the 4-rod $\lambda/2$-resonator and view the multi-sectional "In-line stem 4-rod RFQ" resonator.

to the input impedance of the i-th conductor of the 4CSTL. In order to preserve the voltage and current distribution in the 4CSTL, this equivalent impedance of the supporting posts should be matched with the impedance of the 4CSTL. The input impedance of i-th conductor is defined as $Z_i^{in}=U_i/I_i$. When only a singe normal mode exists in the 4CSTL, the input impedance of all conductors are the same functions on z according to the relations (21) and (19), i.e. $Z_i^{in}=U(z)/I(z)=Z^{in}(z)$. For matching, the input impedance of every supporting post $\tilde{Z}_i^{in}$ has to correspond to the function $Z^{in}(z)$. But practically, it is impossible to make the supporting post to have an arbitrary given absolute values of $\tilde{Z}_i^{in}$. They may be made as mechanically identical ones with the same the $\tilde{Z}_i^{in}$-values. This means that these identical supporting posts should be installed at the same z.

As the results, in the case of 4-rod resonator with single normal modes, the supporting post should be identical and should have in-line arrangement. The shape and configuration of the supporting posts do not influence on mode contents of the cavity modes. Only numerical characteristics of resonators depend on their shapes. The supporting posts can be realized in many configurations. They are based on different systems of conductors, which can produce input impedance with an inductive nature. They range from the simplest straight stems to spiral supports. Probably, it is possible to make the supporting posts on the base of the so-called poly-coaxial resonators[76]. It may be a competitor with spiral supports because of mechanical strengths. Similar construction of support is applied in the drift-tube resonator with two-coaxial support[77].

If above conditions of impedance matching is not satisfied, the operating RFQ mode of 4-rod RFQ resonator will contain an additional non-quadrupole normal modes. Practically, there can be two cases. First case corresponds to the 4-rod RFQ with indentical supporting posts, which are not arranged "In-line". In the second case the supporting posts have no the rotational symmetry for 90°. The presence of non-quadrupole normal modes requires the special consideration for each case.

5.2 *4-rod resonators on the basis of a combination of TEM modes.*

5.2.1 *Dipole modes combinations*

As the examples of the mode combinations, the cases with only the dipole modes are used, because the graphical presentation in such cases is very clear and simple. It is explained by the fact that the distributed parameters of two dipole modes are the same.

Fig. 9 shows the dipole mode combination when two dipole modes with equal amplitudes are summed in-phase. Because the distributed parameters are identical, their voltage and current have the same amplitudes. The left side of the Fig. 9, a shows the initial voltage and current distributions on all conductors of the 4CSTL which correspond exactly to the half-periods of sine and cosine curves, respectively. The results of their summation are given on the right side of the Fig. 9, a. Below it, the resulting resonator corresponding to the shaded $\lambda/4$-section of the 4CSTL is shown.

In this case, one pair of electrodes is excited in opposite phases as two $\lambda/4$-vibrators. The other pair has no current and voltage at any z. Hence, it is not necessary to connect the ends of the non-excited pair of the conductors to the cavity tank.

Fig. 9, b shows the potential signs and the current directions of the electrodes together with field lines at different cross-sections of this resonator. They were derived using the above

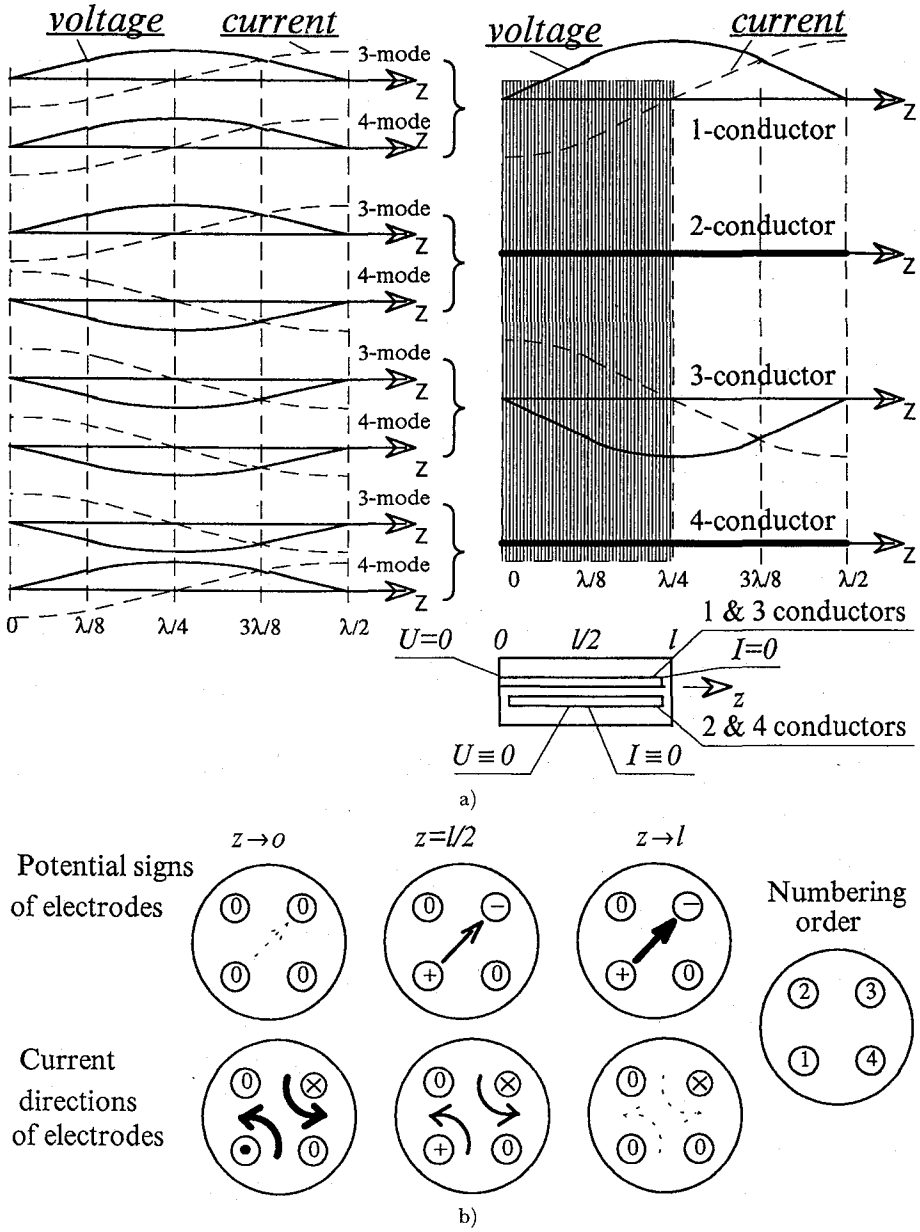

Fig. 9. The cophased superposition of the dipole modes: a) the voltage and current distributions of dipole modes, the voltage and current distributions of the summed TEM wave and the resulting resonator; b) The potential signs and current directions at different cross-sections of the resulting resonator.

distributions in Fig. 9, a. The corresponding field patterns calculated by MAFIA-code are shown in Fig. 10. The results by MAFIA calculations are in a perfect agreement with ones from our method shown in Fig, 9, b. The ratio of the maximum value of the field strength to the value at the middle of the resonator is obtained from sinusoidal distribution to be 0.707 in present method. The corresponding ratio for *E*-fields is equal to 0.71 (=0.67/0.95) and for B-fields 0.72

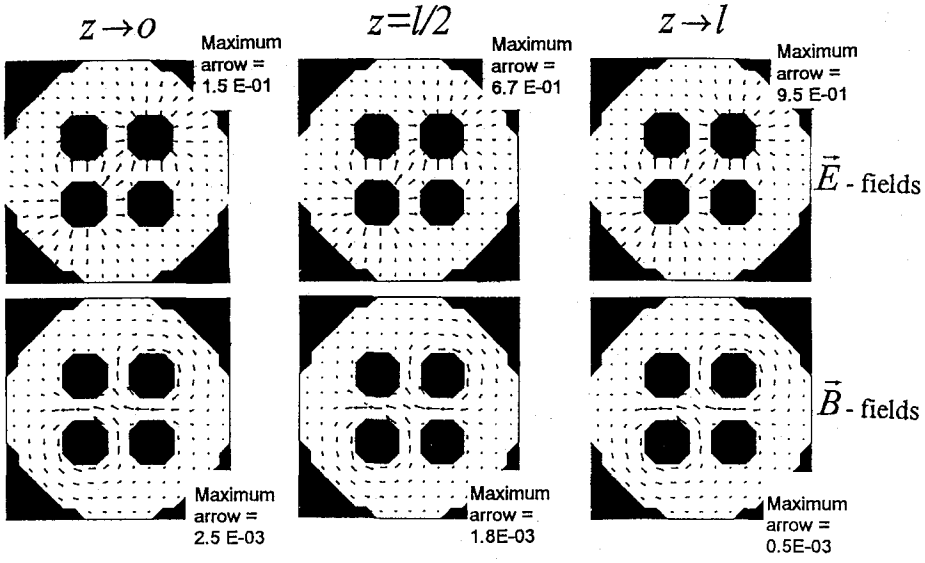

Fig. 10. The field patterns calculated by MAFIA-code for the cophased superposition of the dipole modes shown in Fig. 9.

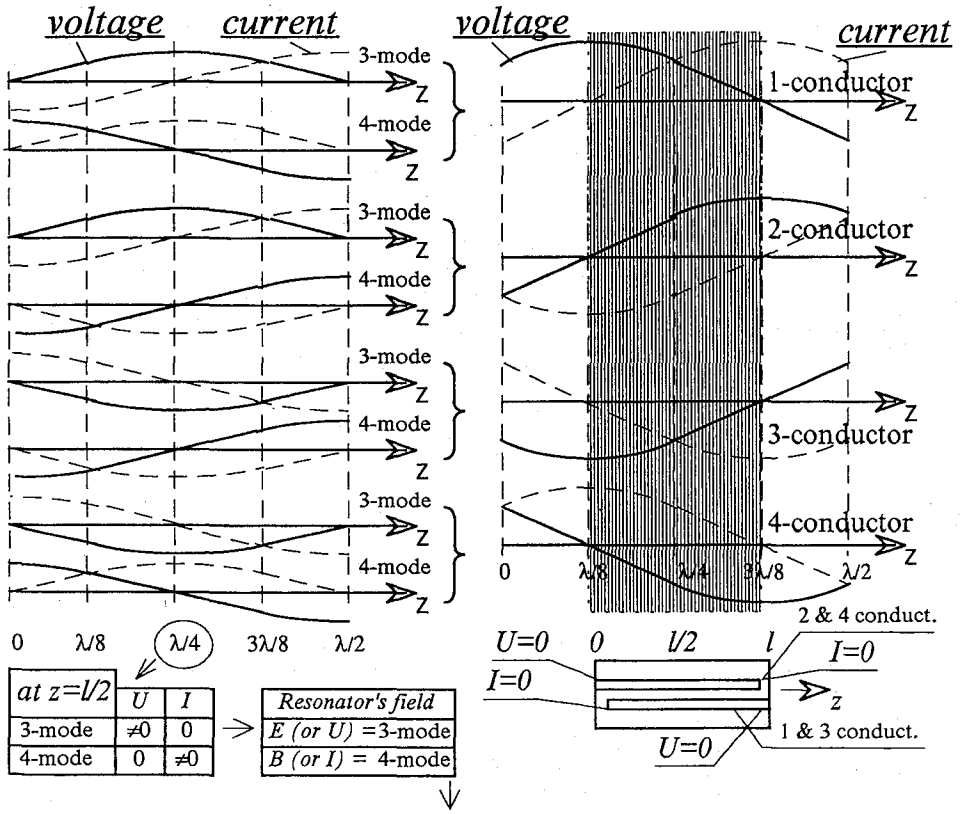

Fig. 11, a)

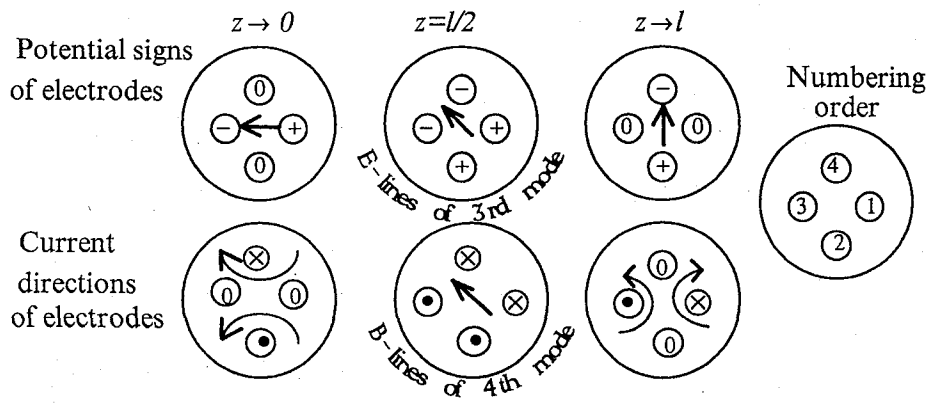

b)

Fig. 11. The superposition of the dipole propagating modes shifted by $\lambda/4$ relative to each other: a) the voltage and current distributions of dipole modes, the voltage and current distributions of the summed TEM wave and the resulting resonator; b) The potential signs and current directions at different cross-sections of the resulting resonator.

(=1.8/2.5) in the case of MAFIA calculation. Thus, our graphical consideration has coincided with 3-D MAFIA-results.

Fig. 11 shows another dipole mode combination when two dipole modes with equal amplitudes are summed in a $\lambda/4$ phase shift. The left side of the Fig. 11, a shows the initial voltage and current distributions on all conductors of the 4CSTL which correspond exactly to the half-periods of sine or cosine curves. The results of their summation are given on the right side of the Fig. 11, a. Below it a schematically drawing of the resulting resonator corresponding to the shaded $\lambda/4$-section of the 4CSTL is shown.

In this case, all electrodes are excited as four $\lambda/4$-vibrators and the system consists of two

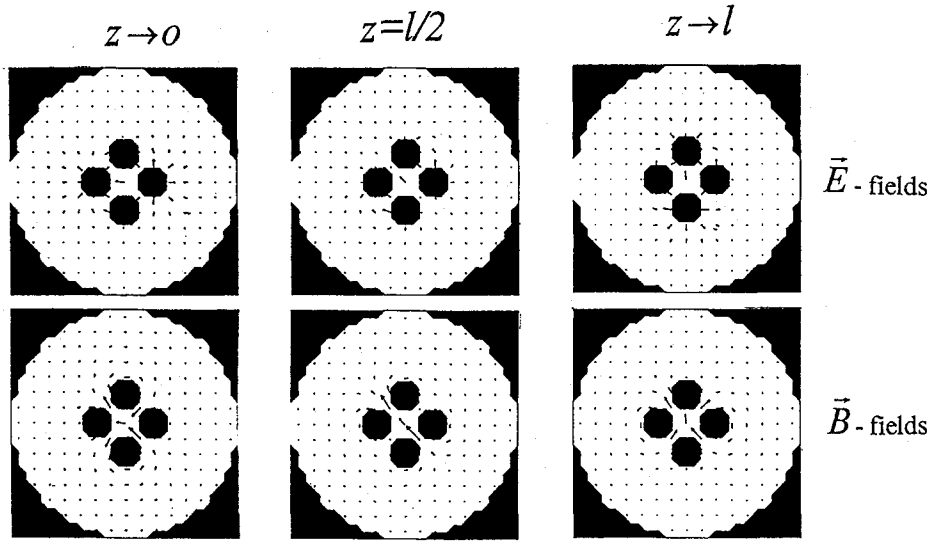

Fig. 12. The field patterns calculated by MAFIA-code for the superposition of the dipole modes shown in Fig. 11.

pairs of the opposing electrodes with the same zero-boundary conditions ($I=0$, $U=0$). Each pair of the opposing electrodes is exited in opposite phases. The both ends of each pair must be connected to the tank in similar way (see Fig. 11, a). This type of the cavity mode exist in the one-section $\lambda/4$-resonator with the alternate arrangement of connections between rods and the tank (Fig. 13, a).

Fig. 11, b shows the potential signs and the current directions of the electrodes together with field lines at different cross-sections of this resonator. They are derived using the above distributions in Fig. 11, a. Because voltage of the 4th mode is equal to zero at the middle of the

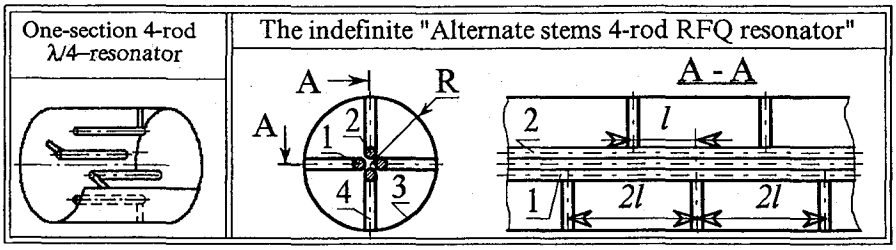

a)

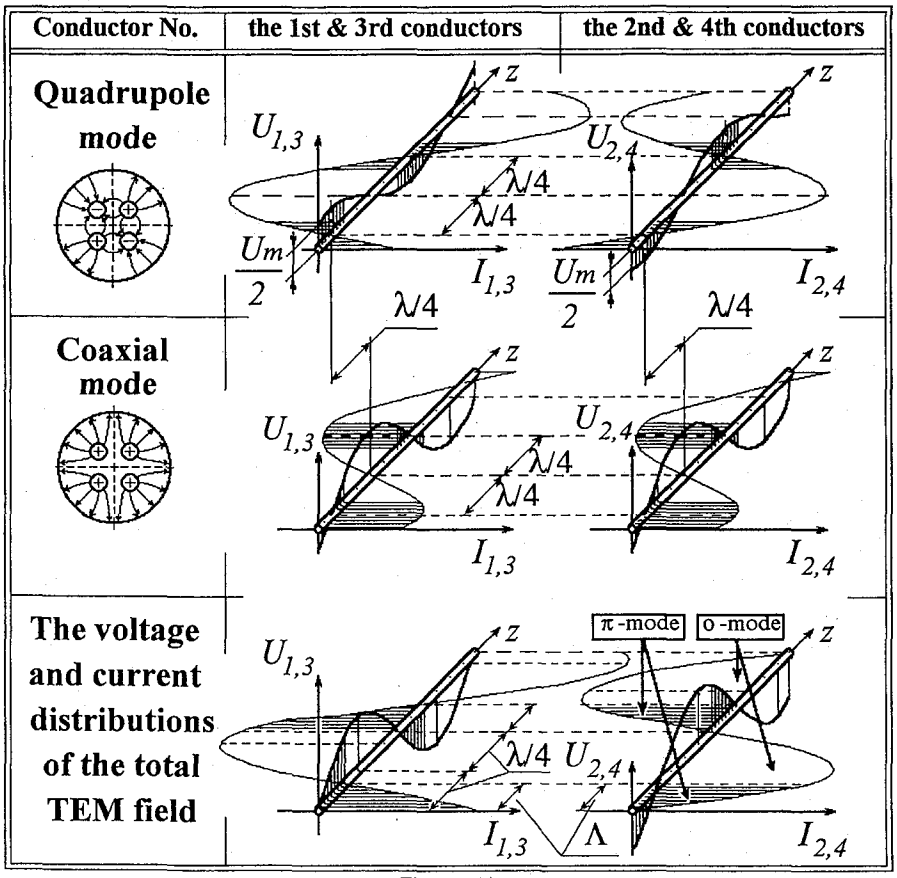

Fig. 13, b)

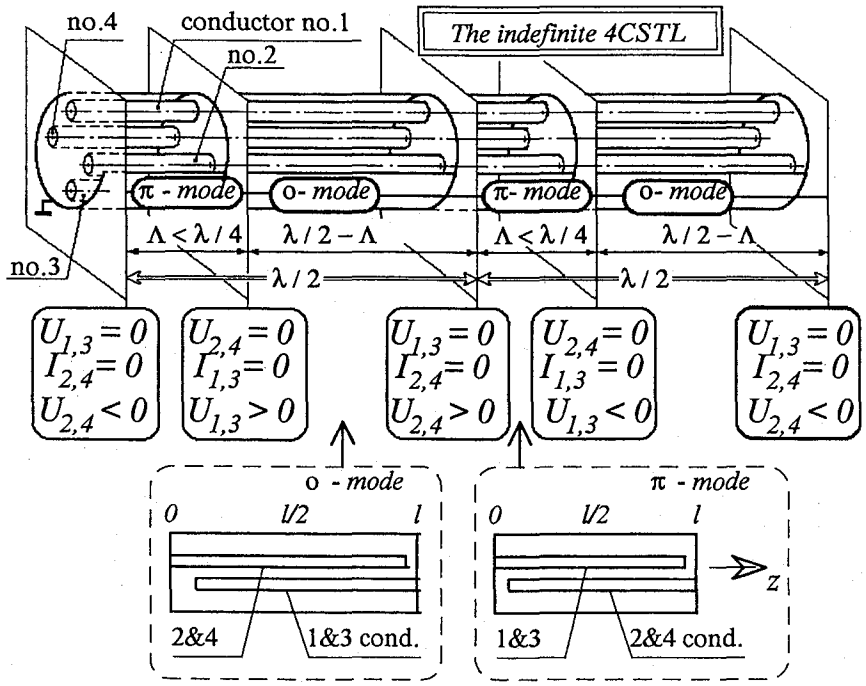

c)

Fig. 13. The mode superposition which corresponds to the "Alternate stems 4-rod RFQ"resonator: a) The views of the one-section $\lambda/4$ resonator and the indefinite multi-sectional resonator; b) The superposition of the quadrupole and coaxial propagating modes shifted by $\lambda/4$ relative each to other; c) The transverse planes of the 4CSTL with zero boundary conditions and resulting resonators for o-mode and π-mode.

resonator, the electric field here comes from only the 3rd mode. The magnetic field at $z=l/2$ is defined only by the 4th mode from the similar reason. The corresponding field patterns calculated by MAFIA-code are shown in Fig. 12. These pictures are in good agreement with ones in Fig, 11, b.

Thus, our graphical consideration can predicate and explain the dipole cavity mode of the 4-rod resonator. The presented examples illustrate also that the current and voltage of propagating modes may be non-zero at open and shorted ends of conductors, respectively. The boundary conditions require the zero values only for corresponding voltage and current of original field.

5.2.2 *Combinations with quadrupole mode*

Now we consider the mode combinations with participant of the quadrupole mode. Because of the difference of distributed parameters between quadrupole mode and any another, it is impossible to get the figures of mode combinations without any calculations as it is done for above cases of dipole modes. To define the voltage and current distributions, we should find the constant coefficients in the solutions (19). They can be derived using zero boundary conditions. In this paper we have omitted the details of these calculations. The results are expressed graphically for qualitative consideration.

A practically important case of the mode combination which corresponds to the one-section of the "Alternate stems 4-rod RFQ resonator" shown in Fig. 13, a is presented in Fig. 13, b. This is the superposition of the standing waves of coaxial and quadrulpole TEM modes shifted along longitudinal direction by $\lambda/4$, while the voltage amplitude of coaxial mode is larger than the quadrupole mode by factor $2(C_1/C_2)^{1/2}$, where C_1 and C_2 are distributed capacitance of the coaxial and quadrupole modes, respectively.

As shown in Fig. 13, b, there is a set of transverse planes perpendicular to the z-axis of the 4CSTL in which either voltage or current on each conductor of the 4CSTL is equal to zero (Fig. 13, c). In these planes, the conductors with zero voltage can be connected to the shield and the conductors with zero current can be cut to open-circuits. The segments between neighboring planes are resonant circuits corresponding to the one-section of the "Alternate stems 4-rod RFQ" resonator. The short segment with length $\Lambda(\Lambda<\lambda/4)$ corresponds to π-mode relative to neighboring rods (RFQ operating mode) and the longer one with length $\lambda/2-\Lambda$ corresponds to 0-mode (in-phase neighboring rods). The sum of the lengths of π and 0 mode segments is equal

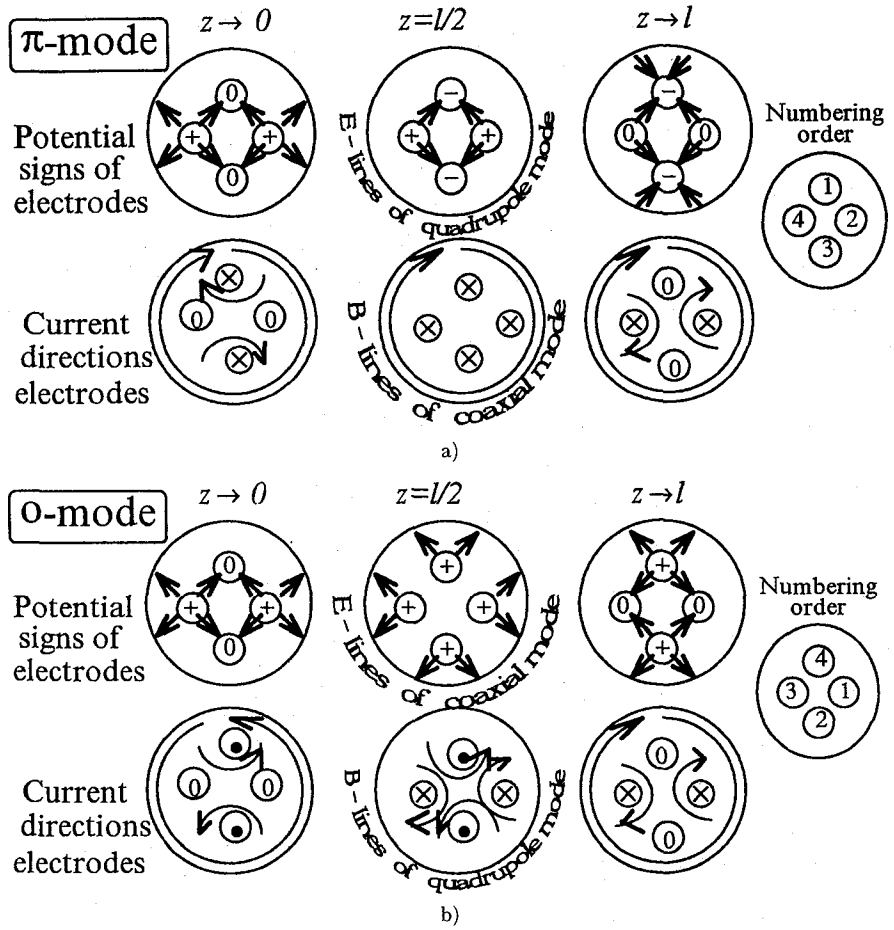

Fig. 14. The potential signs and current directions at different cross-sections of the resulting resonators shown in Fig. 13, c: a) π-mode; b) o-mode.

to exactly $\lambda/2$. It should be noted, that the difference of the segment length from $\lambda/2$ is caused by the difference of the wave impedance between coaxial and quadrupole modes.

In contrast to the quadropole and coaxial mode combination, the above discussed combinations of two dipole modes, which have exactly the same wave impedance, result in the equal segment lengths $\Lambda=\lambda/4$. The dipole resonator modes with the same frequencies are degenerative. Two combinations of coaxial and quadrupole normal TEM modes correspond to π and 0 resonator modes and others correspond to different combinations of two dipole modes. For the unit section with length l it can be obtained that $f_\pi+f_0=2f_d$, where $f\pi$, f_0 and f_d are frequencies of π-mode, 0-mode and dipole modes, respectively, while $f_d\approx(\nu/4l)$, where ν is velocity of light.

Fig. 14 shows the potential signs and the current directions of the electrodes together with field lines at different cross-sections of this resonator for π and 0 resonator modes. They are derived using the above distributions in Fig. 13, b, c. The corresponding field patterns calculated by MAFIA-code are shown in Fig. 15, a, b. These figures are in agreement with the results of our theory. At the cross-sections corresponding to the middle of the resonator for both modes, we can see the typical patterns of the propagating normal modes.

At open ends of electrodes the currents of two propagating modes have non-zero values. They are compensated and the summed current is equal to zero. Because the current of modes are distributed in the transverse cross-section by different ways, the power losses are non-zero at the open ends of electrodes. This situation is in contrast to the usual case (for example, coaxial

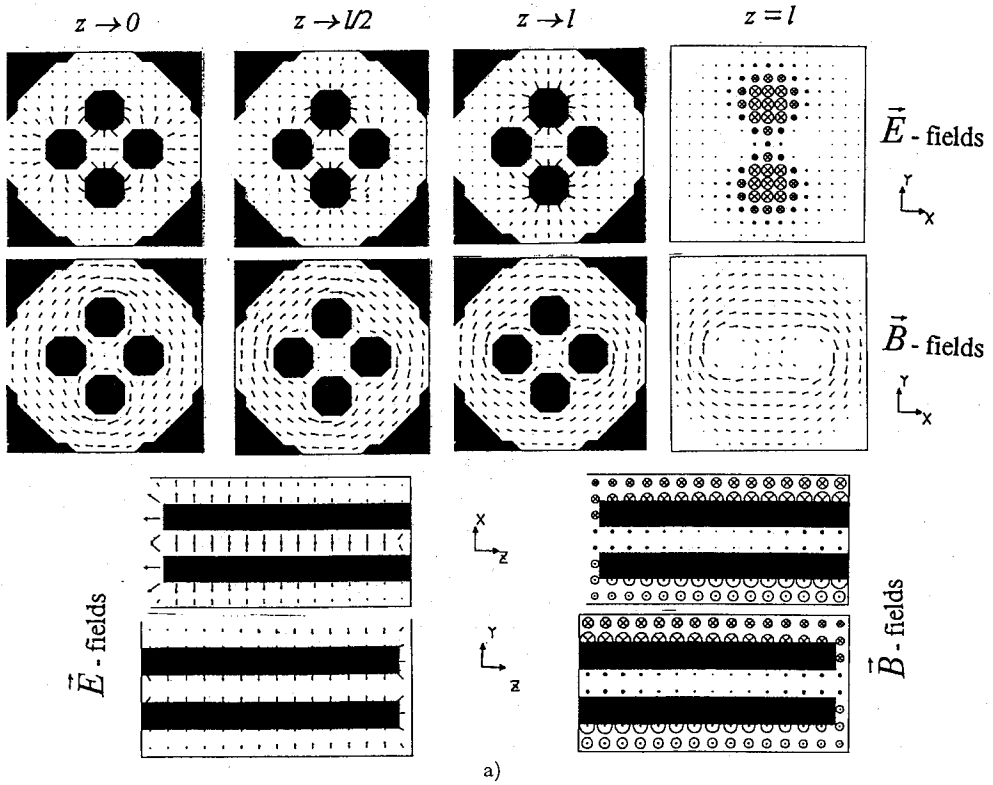

a)

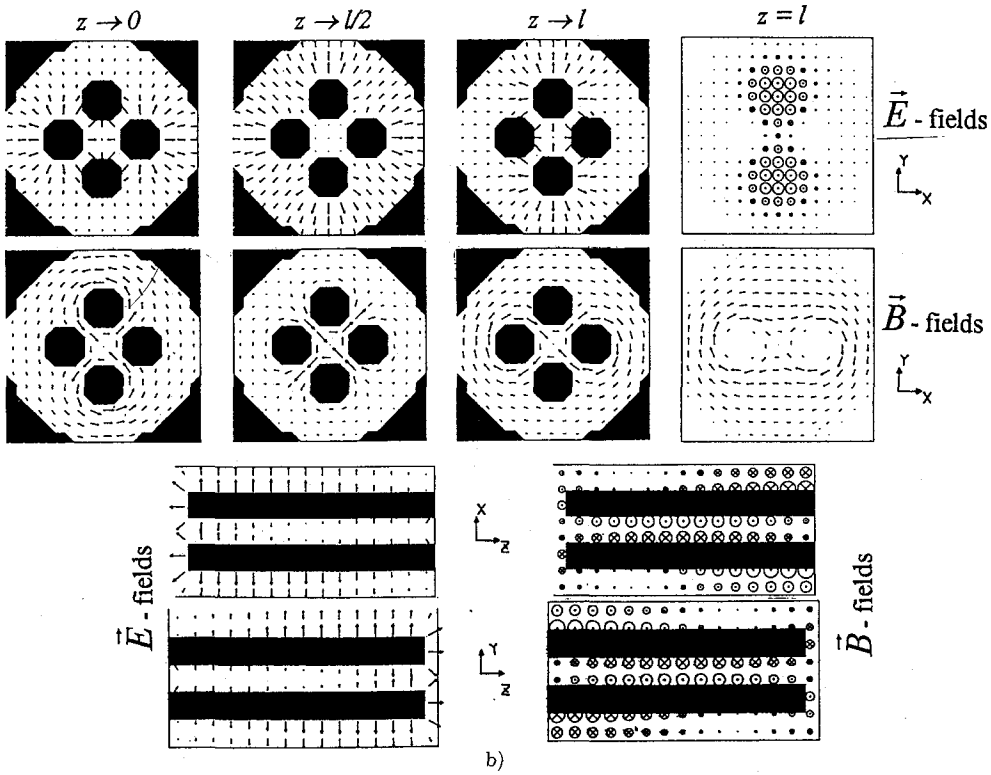

Fig. 15. The field patterns calculated by MAFIA-code for superposition of the quadrupole and coaxial modes shown in Fig. 13 and Fig. 14: a) π-mode; b) o-mode.

resonator or above resonators based on a single mode) in which the power loss at the open end of electrodes is zero.

The cophased superposition of coaxial and qudrupole TEM modes with the same voltage amplitudes results in the $\lambda/4$-resonator as shown in Fig. 16, a. One pair of the electrodes has the zero (as shield) potential and the other one has the voltage distribution which is sinusoidally increasing along z-direction. The results from MAFIA calculations for this resonator are shown in Fig. 16, b. They agree with our consideration. The combination of this $\lambda/4$-resonator with the "Alternate stems 4-rod RFQ" resonator causes a modified resonator, which has an initial part

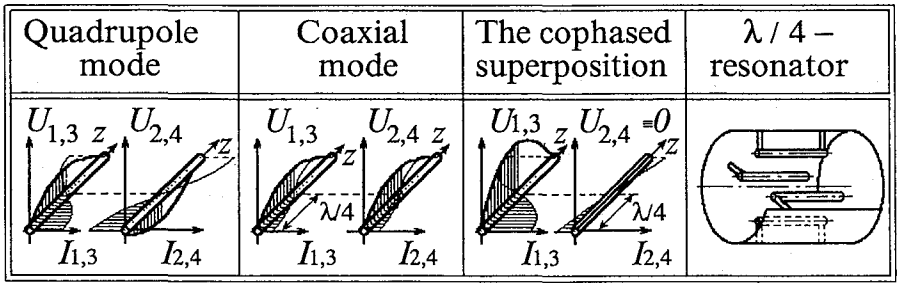

Fig. 16, a)

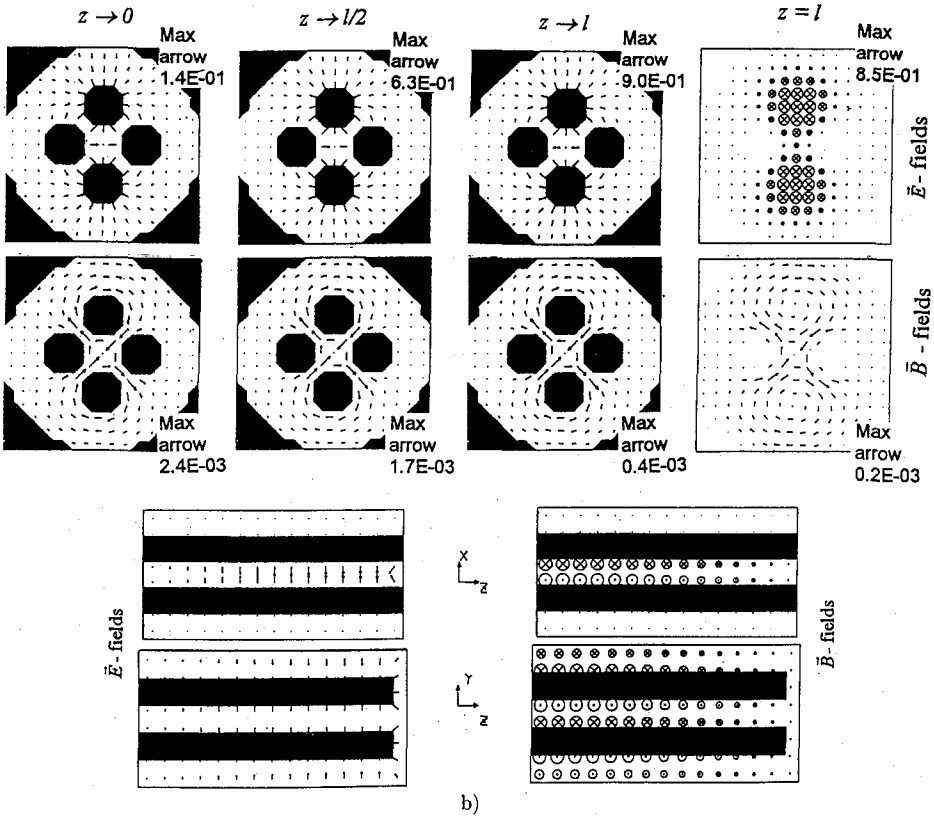

Fig. 16. The cophased superposition of the quadrupole and coaxial modes: a) the present method; b) The field patterns calculated by MAFIA-code.

with increasing RFQ voltage[63]. This initial part can be used as a matching section which is free from undesirable longitudinal fields and has no complicated electrode configuration.

REFERENCES

(1) H. Klein, "Development of the different RFQ accelerating structures and operation experience", *IEEE Trans. Nucl. Sci.*, vol. **30**, No. 4, pp. 3313–3322 (1983).
(2) R.W. Muller, "Layout of a High-Intensity Linac for Very Heavy Ions with RFQ Focusing", *GSI report* **79**-7 (1979).
(3) R.W. Muller, "Work on RF Quadrupole Focusing Structures at GSI", Proc. 1979 L.A.C., *BNL*-**51143**, p. 148–151 (1980).
(4) A. Moretti, *et al.*, "Low frequency RFQ linacs for heavy-ion fusion", Proc. 1981 L.A.C., Santa Fe, *LA*-**9234**, pp. 197–199 (1981).
(5) H. Klein, *et al.*, "Properties of a 0-mode RFQ structure and recent experimental results", Proc. L.A.C., pp. 96–98 (1981).
(6) R.W. Muller, *et al.*, "Proton model of a heavy-ion RFQ linac", *IEEE Tr. NS*-**28**, No. 3, pp. 2862–2864 (1981).
(7) Y. Katayama and H. Takekoshi, "RF Characteristics of Coupled Split Coaxial Lines for RFQ Structure", *Bull. Inst. Chem. Res., Kyoto Univ.*, Vol. **61**, No. 1, pp. 1–11 (1983).
(8) S. Arai, "Split coaxial RFQ structure with modulated vanes", *GSI-report*, GSI-**83**-11 (1983).
(9) R.H. Stokes, *et al.*, "A spiral-resonator Radio-Frequency Quadrupole Accelerator Structure", *IEEE Tr.*

NS-**30**, No. 4, pp. 3530–3533 (1983).
(10) R.M. Hutcheon, "A Modeling Study of the Four-Rod RFQ", Proc. of the 1984 L.A.C., Darmstadt, pp. 94–96 (1984).
(11) S. Arai, *et al.*, "Split coaxial RFQ structure with modulated vane", Proc. of the 5th Symposium on Acc. Sci. and Technology, KEK, pp. 92–94 (1984).
(12) W. Neuman, *et al.*, "Development of split coaxial heavy ion RFQ accelerators", Proc. L.A.C., pp. 80–82, (1984).
(13) A. Schempp, *et al.*, "Four-Rod-λ/2-RFQ for Light Ion Acceleration", *Nucl. Instr. Meth.*, **B10/11**, pp. 831–834, (1985).
(14) E. Tojyo, *et al.*, "A Multi-Module Cavity Structure of Split coaxial RFQ", L.A.C., pp. 374–376 (1986).
(15) P. Leipe, *et al.*, "High Current RFQ accelerator using a split coaxial resonator with a four rod structure", LAC-86, pp. 311–314.
(16) I.M. Kapchinskiy, *et al.*, "RF Linac for Heavy ion fusion driver", LAC-86, pp. 318–322.
(17) T. Ogawa and Y. Iwashita, "Model Study of a 4-rod Sructure of RFQ Linac", *Bull.Inst.Chem.Research, Kyoto Univ.*, Vol. **65**, No. 1, pp. 51–58 (1987).
(18) A. Schempp, *et al.*, "A light ion four rod RFQ injector", Proc of the P.A.C., pp. 267–269 (1987).
(19) S. Arai, *et al.*, "A proton accelerating model of uranium RFQ", PAC-87, pp. 270–272.
(20) M.J. Browman, *et al.*, "Studies of the Four-Rod RFQ using the MAFIA codes", Proc. of the L.A.C., pp. 119–121 (1988).
(21) R. Kazimi, "A 4-rod RFQ cavity RFQ", LINAC-88, pp. 140–142.
(21a) R. Kazimi, "Study of a Four-rod RFQ structure at 470 MHz", PAC-89, pp. 990–992.
(21b) R. Kazimi, *et al.*, "Test of a 473 MHz Four-rod RFQ", *LA*C-90, pp. 698–670.
(22) A. Fabris and A. Massarotti, "Proposal for a Variable Energy RFQ", *N.I.M.*, **A273**, pp. 1–4 (1988).
(23) N. Tokuda, *et al.*, "Structure and RF Characteristics of the INS 25.5 MHz Split coaxial RFQ", Proc. of the 7th Symposium on Acc. Sci. and Techn, pp. 92–94 (1989).
(24) H. Fujisawa, *et al.*, "4-rod RFQ Proton Acceleration Tests", *Bull. Inst. Chem. Res., Kyoto Univ.*, Vol. **67**, No. 1, pp. 7–14 (1989).
(24a) H. Fujisawa, *et al.*, "Design Study of a heavy Ion RFQ Linac", *Bull. I.C.R., Kyoto Univ.*, Vol. **68**, No. 2, pp. 121–126 (1990).
(25) A. Schempp, "Variable energy and heavy ion RFQs", Proc. L.A.C., p. 535–539 (1990).
(26) I. Ben-zvi, *et al.*, "Electrical Characteristics of a short RFQ resonator", *LA*C-90, pp. 73–75.
(27) H. Wang, *et al.*, "Numerical simulation of a short RFQ Resonator Using the MAFIA Codes", P.A.C., pp. 3038–3040 (1991).
(28) H. Fujisawa, *et al.*, "Mechanical Design of 33.3 MHz 4-Rod Heavy Ion RFQ Cavity", *Bull. Inst. Chem. Research, Kyoto Univ.*, Vol. **70**, No. 1, pp. 28–36 (1992).
(29) Chen Chia-Erh, *et al.*, "Layout and High Power Test of a 26MHz Spiral RFQ", Proc. EPAC, pp. 1328–1331 (1992).
(30) A. Lombardi, *et al.*, "Comparison Study of RFQ Structures for the Lead-Ion 4-rod RFQ at the CERN", EPAC, pp. 557–559 (1992).
(31) A. Schempp, "The Application of RFQ's", Proc. L.A.C., Ottawa, pp. 545–549, (1992).
(32) V.A. Andreev, *et al.*, "Analysis of the End Regions of the CERN Lead-Ion 4-rod RFQ", IEEE P.A.C., Vol. .4, pp. 3121–3123 (1993).
(33) V.A. Andreev, G. Parisi. "90°-apart-stem RFQ Structure for wide Range of Frequencies", IEEE P.A.C., Vol. 4, pp. 3124–3126 (1993).
(34) J.R. DeLayen, *et al.*, "Design considerations for High-current Superconducting RFQ's", IEEE P.A.C., Vol. 2, pp. 838–890 (1993).
(35) H. Fujisawa, "A cw 4-rod RFQ linac", *N.I.M.*, **A345**, pp. 23–42, (1994).
(36) V.A. Andreev and G. Parisi, "Field Stabilization and End-Cell Tuning in a 4-vane RFQ", E.P.A.C., pp. 1300–1302 (1994).
(37) M. Grieser, *et al.*, "Status of the Heidelberg High Current Injector", LINAC-94, Tsukuba, pp. 698–700.
(38) B. Bondarev, *et al.*, "Development and study of the opposed vibrator resonator for RFQ comact ion linacs", E.P.A.C., pp. 1337–1339 (1992).
(39) A. Schempp, *et al.*, "Zero-mode-RFQ development in Frankfurt", Proc. L.A.C., Darmstadt, pp. 100–102, (1984).
(40) R.W. Muller, *et al.*, "Experimental Results with a Very-Heavy-Ion RFQ Accelerating Structure at GSI", LINAC-84, pp. 77–79.
(41) S. Arai, "Analysis of a multi-module split coaxial RFQ", Inst. Nucl. Study, Tokyo, techn. report INS-T-

464, November (1986).
(42) A. Schempp, *et al.*, "The Crying RFQ", LINAC-88, pp. 70–72 ; A.Schempp, "Recent progress in RFQ", LINAC-88, pp. 460–462.
(43) J.X. Fang and A. Schempp, "Equivalent circuit of a 4-rod RFQ", Proc. EPAC, p. 1331–1333 (1992).
(44) I. Ben-zvi, *et al.*, "Design of a Superconducting RFQ Resonator", *Part. Acc.*, Vol. **35**, pp. 177–192 (1991).
(45) V.A. Andreev, *et al.*, "Developent of a radioactive nuclides accelerator at the Moscow meson factory", PAC-91, pp. 2984–2986.
(46) S. Arai, *et al.*, "Development of an SCRFQ heavy-ion linac for RI beams", *N.I.M*, B**70**, pp. 414–420 (1992).
(47) E.L. Ginzton, "Microwave Measurements", by McGraw-Hill Book Company, Inc., pp. 313 (1957).
(48) R.M. Hutcheon, "An Equivalent circuit model of the general 3-dimensional RFQ", P.A.C., *IEEE Tr.* **NS-30**, No. 4, pp. 3524–3527 (1983).
(49) V.V. Kapin, "The Analysis of the RFQ multi-rod accelerated structures", In : 1991 All-Union Linear Accelerator Seminar, Thesis of reports, Kharkov, p. 61 (1991) (in Russian).
(50) V. Kapin, "Study of the Four-Rod RFQ Using the Normal Mode Theory of Transmission Lines", EPAC, pp. 2191–2193 (1994).
(51) M.S. Livingston and J.P. Blewett, Particle accelerators, by McGraw-Hill Book Company, Inc., pp. 336 (1962).
(52) G. Nassibian, *et al.*, "A One-MeV/nucleon Sloan and Lawrence heavy-ion linear accelerator", *Rev.Sci.Instr.* Vol. **32**, pp. 1316 (1961).
(53) C. Bieth, *et al.*, "A One-MeV/nucleon heavy-ion linear accelerator", Proc. L.A.C., pp. 508–510 (1966).
(54) "Linear Accelerators", Ed. by P.M. Lapostole and A.L. Septier, Amsterdam, pp. 710, 1058 (1970).
(55) J. Pottier, "Heavy ion accelerating structure and its application to a heavy-ion linear accelerator", United States Patent 4,181,894, Foreign Application Priority Data, May 5 (1977).
(56) V.K. Baev and V.P. Zubovskiy, "Accelerating system", USSR author's certificate No. 586780. Bulletin OIPOTZ, No. 10, c. 297 (1982) (in Russian).
(57) V.M. Pirozenko and I.B. Seleznev, "The accelerating structure with the opposed vibrators", Proc. of Moscow Radiotechnical Institute, No. 39, pp. 3–13, (1980) (in Russian).
(58) I.M. Kapchinskiy, "Theory of resonance linear accelerators", Harwood (1985).
(59) O.V. Plink, "Dispersion equations for accelerating structures using branched coaxial and bifilar shielded transmission lines", *Sov. Journ. Techn. Phys*, **28**(4), 491–492 (1983).
(60) V.V. Kapin, Report's Annotations of the 11 USSR Linac Seminar, Kharkov, p. 39 (1989) (in Russian).
(61) V.V. Kapin, "The resonance Equivalent Resistance and Quality of the one-section of multi-conductor cavity for RFQ accelerator", In: Trans. on Radiation Acceletation Complexes, Ed. by B. Ju. Bogdanovich and V.P. Kozlov, Moscow Engineering Physics Institute, pp. 49–58 (1991) (in Russian).
(62) V.V. Kapin, *et al.*, "Proton prototype of accelerator of multi-charged ions with variable energy of accelerated particles", In : 1991 All-Union Linear Accelerator Seminar, Thesis of reports, Kharkov, pp. 115 (1991) (in Russian).
(63) V. Kapin, M. Inoue, Y. Iwashita and A. Noda, "Normal Mode Analysis of the Four Rod RFQ As a System of TEM Transmission Lines", Proc. LINAC-94, pp. 254–256.
(64) R.E. Collin, "Field Theory of Guided Waves", McGraw-Hill, Inc. (1960).
(65) C.C. Johnson, "Field and wave electrodynamics", McGraw-Hill Inc. (1965).
(66) A.D. Grigorjev, "Electrodimamika i tehnika S.V. Ch" (Electrodynamics and RF Technique), M., Vish. shk. (1990) (in Russian).
(67) J.R. Carson and R.S. Hoyt, "Propagation of periodic currents over system of parallel wires", *Bell. Syst. Techn. Journ.*, Vol. **6**, No. 3, 435–545 (1927).
(68) S.I. Baskakov, "Radiotechnical curcuits with distributed parameters", Moscow, Vish. Schola (1980) (in Russian).
(69) M.V. Kostenko, *et al.*, "The wave processes and electric noises in the high-voltage multi-conductor lines", Moscow, Energiya, (1973) (in Russian).
(70) Handbook of physics, Second edition, ed. by E.U. Condon and H. Odishaw, McGraw-Hill Book Co., pp. 4–20, 4–21, 4–24 (1967).
(71) W.R. Smythe, "Static and dynamic electricity", McGraw-Hill Book Co., p. 37 (1950).
(72) Yu. Ya. Iossel, "The calculation of electrical capacity", Leningrad, Energoizdat (1981) (in Russian).
(73) G.P. Harnwell, "Principles of electricity and electromagnetism", McGraw-Hill Book Co., pp. 322 (1949).
(74) S. Koscielniak, "Analitic Study of Transverse Shunt Resistance and Even-Odd Mode Coupling of a Rod

Type RFQ", EPAC, pp. 2188–2190 (1994).
(75) R. Klatt, *et al.*, "MAFIA—A Three-dimensional Electromagnetic CAD System for Magnets, RF Structures and Transient Wake-field Calculations", Proc. L.A.C., Stanford, pp. 276–278 (1986).
(76) F.A. Vodopianov, "Polycylindrical resonators in the accelerating technique", EPAC, pp. 2121–2123 (1994).
(77) K. Yoshida, *et al.*, "Model test of a double-coaxial $\lambda/4$ resonant cavity as a rebuncher", Proc. LINAC-94, pp. 771–773.